Title

Glucose sensor O-GlcNAcylation coordinates with phosphorylation to regulate circadian clock.

Journal

Cell metabolism, 17(2)

ISSN

1550-4131

Authors

Kaasik, Krista
Kivimäe, Saul
Allen, Jasmina J
et al.

Publication Date

2013-02-01

DOI

10.1016/j.cmet.2012.12.017

Peer reviewed

Volume 17
Number 2

February 5, 2013

www.cellpress.com

Cell Metabolism

O-GlcNAcylation and Circadian Clock

Cell Metabolism
Article

Glucose Sensor *O*-GlcNAcylation Coordinates with Phosphorylation to Regulate Circadian Clock

Krista Kaasik,[1] Saul Kivimäe,[2,7] Jasmina J. Allen,[3,7] Robert J. Chalkley,[4] Yong Huang,[1] Kristin Baer,[6] Holger Kissel,[6] Alma L. Burlingame,[4] Kevan M. Shokat,[3,5] Louis J. Ptáček,[1,5,*] and Ying-Hui Fu[1,*]
[1]Department of Neurology
[2]Department of Bioengineering and Therapeutic Sciences
[3]Department of Cellular and Molecular Pharmacology
[4]Department of Pharmaceutical Chemistry
[5]Howard Hughes Medical Institute
University of California San Francisco, San Francisco, CA 94158, USA
[6]TaconicArtemis GmbH, 51063 Cologne, Germany
[7]These authors contributed equally to this work
*Correspondence: ljp@ucsf.edu (L.J.P.), ying-hui.fu@ucsf.edu (Y.-H.F.)
http://dx.doi.org/10.1016/j.cmet.2012.12.017

SUMMARY

Posttranslational modifications play central roles in myriad biological pathways including circadian regulation. We employed a circadian proteomic approach to demonstrate that circadian timing of phosphorylation is a critical factor in regulating complex GSK3β-dependent pathways and identified *O*-GlcNAc transferase (OGT) as a substrate of GSK3β. Interestingly, OGT activity is regulated by GSK3β; hence, OGT and GSK3β exhibit reciprocal regulation. Modulating *O*-GlcNAcylation levels alter circadian period length in both mice and *Drosophila*; conversely, protein *O*-GlcNAcylation is circadianly regulated. Central clock proteins, Clock and Period, are reversibly modified by *O*-GlcNAcylation to regulate their transcriptional activities. In addition, *O*-GlcNAcylation of a region in PER2 known to regulate human sleep phase (S662–S674) competes with phosphorylation of this region, and this interplay is at least partly mediated by glucose levels. Together, these results indicate that *O*-GlcNAcylation serves as a metabolic sensor for clock regulation and works coordinately with phosphorylation to fine-tune circadian clock.

INTRODUCTION

Circadian rhythms in physiology and behavior are present in a variety of organisms from plants and bacteria to humans. These rhythms are controlled by endogenous molecular clocks even in the absence of external cues (e.g., light). The fact that circadian clocks are evolutionarily conserved supports the view that precise rhythms are essential for organisms to survive. Perturbations of circadian rhythms and sleep have been associated with many human ailments such as metabolic syndrome, cardiovascular disease, depression, epilepsy, and cancer (Bass and Takahashi, 2010; Climent et al., 2010; Duez and Staels, 2010; Wulff et al., 2010).

Glycogen synthase kinase 3β (GSK3β) is an important signaling mediator that has central functions in diverse physiological pathways including transcription, cell-cycle regulation, metabolism, development, neuronal function, and oncogenesis, among others (Rayasam et al., 2009). These diverse functions of GSK3β can be attributed to the large number of substrates it can phosphorylate. GSK3β is a constitutively active serine/threonine kinase with a preference for primed substrates and is inactivated in response to multiple stimuli by phosphorylation at S9 (Cohen and Frame, 2001). GSK3β is also a crucial circadian clock regulator (Iitaka et al., 2005; Martinek et al., 2001). Lithium (a GSK3β inhibitor) treatment lengthens the circadian period and delays the phase of rhythmic clock gene expression (Abe et al., 2000; Iitaka et al., 2005), although a recent report showed that inhibition of GSK3β activity by small molecule inhibitors or siRNAs shortens the circadian period (Hirota et al., 2008). In order to further understand the effects of GSK3β activity on various biological pathways in general and circadian regulation in particular, we employed a proteomic approach to elucidate the complexity of the GSK3β circadian phosphoproteome. Interestingly, we identified *O*-GlcNAc transferase (OGT) from the chemical-genetic proteomic screen as a substrate of GSK3β. GSK3β was previously shown to be *O*-GlcNAcylated by OGT in vitro (Lubas and Hanover, 2000). Since our data suggest that OGT and GSK3β regulate each other and GSK3β is a critical molecular clock component, we investigated the possibility of *O*-GlcNAcylation as a regulatory posttranslational modification in circadian regulation.

O-linked N-acetylglucosamine (*O*-GlcNAc) glycosylation has emerged as one of the most common protein posttranslational modifications with the second most abundant high-energy compound, UDP-GlcNAc, as the direct donor. Two enzymes regulate *O*-GlcNAcylation: the OGT attaches UDP-GlcNAc to the serine and threonine residues of proteins through a beta-glycosidic *O*-linkage, while *O*-GlcNAcase (OGA) hydrolyzes *O*-GlcNAc from proteins (Hart et al., 2011). OGT and OGA are highly regulated to prevent unnecessary *O*-GlcNAc cycling (Sekine et al., 2010). Here we report that *O*-GlcNAcylation and circadian clock are reciprocally regulated and that *O*-GlcNAcylation modulates CLOCK-dependent transcriptional activity by post-translationally regulating components of the molecular clock.

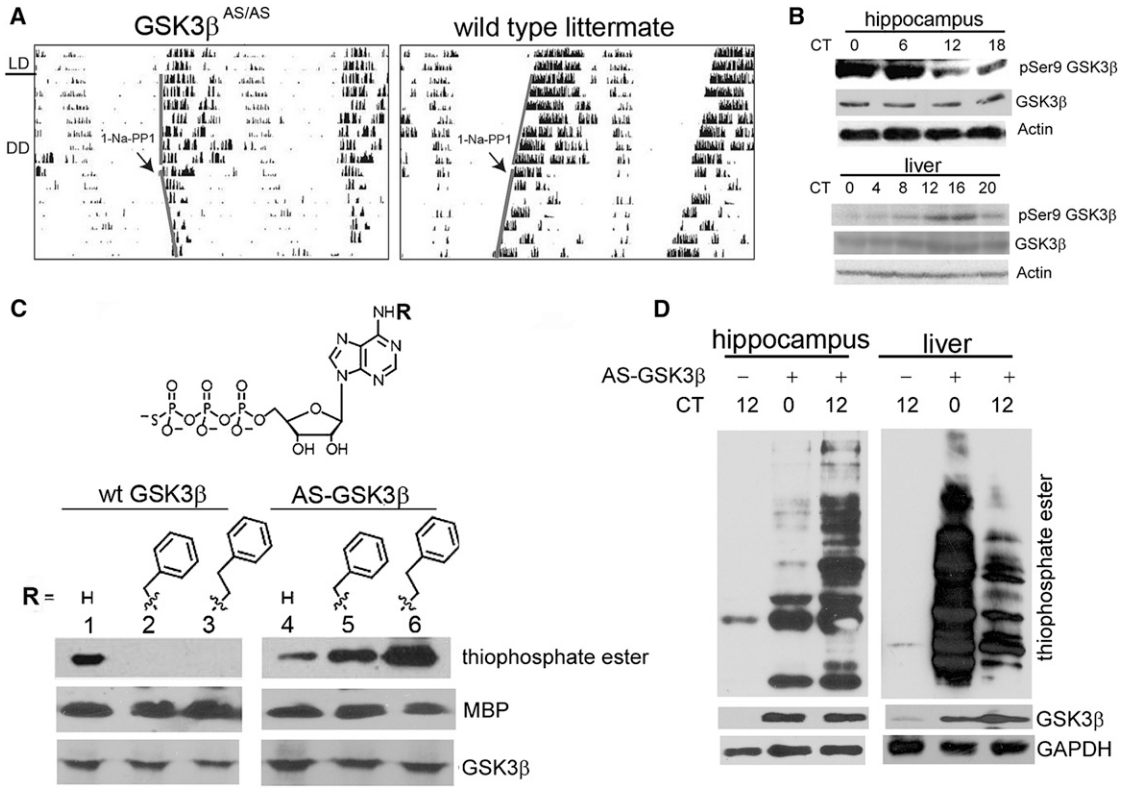

Figure 1. Characterization of GSK3β by ATP Analog-Specific Chemical-Genetic Method

(A) Representative double-plotted actograms of daily wheel-running activity for GSK3β$^{AS/AS}$ and WT littermate mice. 1-Na-PP1 treatment was initiated after 1 week in constant darkness and administered daily for a week. The arrow on each actogram indicates the beginning of inhibitor treatment. 1-Na-PP1 treatment lengthens the circadian period of GSK3β$^{AS/AS}$ mice in constant darkness from $\tau = 24.0 \pm 0.12$ hr (no inhibitor; n = 10) to $\tau = 24.5 \pm 0.1$ hr (with inhibitor; n = 6, $p < 0.01$). 1-Na-PP1 treatment does not affect circadian period length in WT littermates ($\tau = 23.7 \pm 0.15$ hr [no inhibitor; n = 10] versus $\tau = 23.5 \pm 0.07$ hr [with inhibitor; n = 6]).

(B) Western blot demonstrates that pS9 of GSK3β oscillates at different phases in different tissues with the phase of hippocampus antiphase to the phase of liver.

(C) In vitro kinase reactions show that WT GSK3β is unable to utilize N-6-modified ATPγS analogs (lanes 2 and 3) as phosphodonors but utilizes ATPγS (lane 1). AS GSK3β (L132G) efficiently utilizes both unmodified (lane 4) and N-6-modified ATPγS analogs (lanes 5 and 6) and prefers N-6-phenethyl ATPγS (lane 6). Loading controls for the substrate myelin basic protein (MBP) and GSK3β are included.

(D) GSK3β demonstrates antiphase phosphorylation of substrates in hippocampal versus liver tissue. AS GSK3β kinase was added to the protein extracts, and kinase assays were performed in the presence of N-6-phenethyl ATPγS. After PNBM alkylation, western blot analysis was performed using the antibodies indicated. Blots for glyceraldehyde phosphate dehydrogenase (GAPDH) demonstrate equal loading. See also Figures S1, S2, and S7 and Tables S1, S2, and S3.

In addition, *O*-GlcNAcylation interplays with phosphorylation on PER2, which likely plays a role in fine-tuning clock speed.

RESULTS

Rhythmic Phosphorylation of GSK3β Substrates

We developed an ATP analog-specific (AS) chemical-genetic approach to identify direct GSK3β substrates that are involved in circadian regulation and coupling of core clock components to input-output pathways. To verify the effect of GSK3β on the circadian clock in vivo, we obtained AS GSK3β knockin mice (GSK3β$^{AS/AS}$, TaconicArtemis). Using analogs of the general kinase inhibitor (PP1) that specifically inhibit AS, but not wild-type (WT) kinases, kinase activity can be specifically, rapidly, and reversibly inhibited (Bishop et al., 2000). Wheel-running activity of GSK3β$^{AS/AS}$ mice was analyzed after entrainment in a 12 hr light/12 hr dark cycle (12L/12D) for 1 week. These mice showed a statistically significant lengthening of period versus WT controls (24 versus 23.7 hr) in constant darkness (DD) (Figure 1A), suggesting that the engineered mutation produces an AS GSK3β kinase with altered enzyme activity. This is consistent with the observation that AS GSK3β enzyme activity is reduced when compared with WT GSK3β by an in vitro kinase assay (Figures S1A and S1B). AS GSK3β is inhibited by the 1-Na-PP1 inhibitor both in vitro in a concentration-dependent manner (Figure S1C) and in vivo (Figure S1E), whereas WT GSK3β is not affected by 1-Na-PP1. Interestingly, after treatment with the AS GSK3β inhibitor (1-Na-PP1), the period was further lengthened to 24.5 hr (versus 24 hr in GSK3β$^{AS/AS}$ without inhibitor; Figure 1A). This finding is congruent with previous data using lithium (Abe et al., 2000; Duez and Staels, 2008). Since lithium acts on targets other than GSK3β (O'Brien and Klein, 2009), the data from the GSK3β$^{AS/AS}$ mice suggest that specific inhibition of GSK3β leads to lengthening of the circadian period.

GSK3β S9 phosphorylation (inactive GSK3β) demonstrates robust circadian oscillation (Iitaka et al., 2005). In order to test

the oscillation of GSK3β S9 phosphorylation in both brain and peripheral tissues, hippocampus and liver tissues were obtained from WT mice (Figure 1B). Hippocampus was used instead of suprachiasmatic nucleus (SCN) due to the ease of anatomical dissection and the need to obtain a sufficient quantity of tissue for proteomic analysis. Phosphorylation of GSK3β S9 in hippocampus peaks at subjective morning (circadian time [CT] 0, lights on or "dawn" in the light/dark cycle) and is antiphase to liver where it peaks at subjective evening (CT12, lights off or "dusk" in the light/dark cycle), consistent with previous findings that kinases demonstrate tissue-specific and time-specific activities (Kategaya et al., 2012). To analyze whether GSK3β activity correlates with the substrates it phosphorylates, we isolated protein extracts from the hippocampus and liver of WT mice at CT0 and CT12. Recombinant AS GSK3β was added to hippocampus and liver protein extracts together with N6-phenethyl ATPγS. AS GSK3β enzyme prefers ATPγS analogs (N6-benzyl ATPγS and N6-phenethyl ATPγS) as thiophospho-donors, whereas these analogs are not accepted by WT GSK3β (Figure 1C). Thiophosphorylated substrates are then alkylated for recognition by a thiophosphate ester-specific antibody (Figures S2A and S2B) (Allen et al., 2005). Substrate phosphorylation patterns by AS GSK3β showed dramatic differences between the two tissues and at different CTs when assessed by western blotting (Figure 1D). The intensity of substrate phosphorylation directly correlated with the GSK3β activity in a circadian manner (the time point with high GSK3β activity in each tissue also showed the highest phosphorylation of substrates).

Analog-Specific GSK3β Substrate Identification

We performed kinase reactions of analog-specific substrate labeling by recombinant AS GSK3β to identify targets from the liver and hippocampus proteomes (at time of peak GSK3β-mediated phosphorylation CT0 in liver and CT12 in hippocampus) (see Figure 1D). This procedure was performed three times with protein extracts from mouse hippocampus and twice with extracts from mouse liver. In the samples with AS GSK3β, 343 and 124 potential GSK3β substrates were identified by mass spectrometry (MS) from the hippocampus and liver, respectively. Eighty-six of these proteins were found in both (Tables S1 and S2). Of the 343 and 124 proteins in these tissues, 145 and 69 of them were found only in samples with AS GSK3β, but not in samples with WT GSK3β, and 30 of them were identified in both the hippocampus and liver (Tables S1 and S3). To validate the effectiveness of this approach, we experimentally examined two proteins, zona occludens protein 1 (ZO1, Figure S2C) and PPP1R9B (Figures 2A and S2D), and confirmed them as substrates of GSK3β. Results from detailed bioinformatic analyses for the proteomic screens can be found in Tables S1, S2, and S3. Proteins identified in the AS GSK3β hippocampus-positive-only and AS GSK3β liver-positive-only were further examined in the Kyoto Encyclopedia of Genes and Genomes (KEGG) database (http://www.genome.jp/kegg) to reveal pathways that are potentially regulated by GSK3β (Figure S7). Many previously known GSK3β-involved pathways, together with additional pathways, were found through this approach, further highlighting the interconnectedness of various regulatory mechanisms. Collectively, these results suggest that daily timing is an important parameter controlling GSK3β substrate specificity and that tissue-specific circadian phosphoregulation of GSK3β substrates may play important roles in the regulation of GSK3β-dependent physiological pathways.

GSK3β Regulates OGT Activity

Intriguingly, OGT was one of the GSK3β substrates that was identified in the chemical-genetic screen (Table S1 and Figure S2E). The covalent dynamic modification of *O*-GlcNAc to proteins by OGT has emerged as a common posttranslational modification that is as abundant as phosphorylation within the nucleus and cytoplasm (Torres and Hart, 1984). To validate OGT as an authentic GSK3β substrate, OGT was immunoprecipitated from brain extracts of WT mice using anti-OGT antibody. The precipitants were then subjected to WT or AS GSK3β kinase reactions with the ATPγS N6-benzyl analog followed by SDS-PAGE, and western blots were probed with thiophosphate ester-specific antibody. In the presence of ATPγS N6-benzyl analog, OGT was phosphorylated by AS GSK3β (Figure 2A). In addition, OGT was phosphorylated by GSK3β using in vitro ^{32}P-labeled ATP (Figure 2B), demonstrating that OGT is a GSK3β substrate.

Mass spectrometry was then employed to identify where GSK3β phosphorylates OGT. OGT, in the presence or absence of GSK3β, was digested with trypsin before the peptides were analyzed by tandem mass spectrometry to identify modified peptides. OGT was found to be phosphorylated on S3 or S4 (data could not distinguish between these potential sites) (Figure 2C, left panel). Extracted ion chromatograms for the intensity of this phosphorylated peptide in the two samples showed a significant increase in the presence of GSK3β, suggesting that this site is modified by GSK3β (Figure 2C, right panel). Interestingly, MS analysis also revealed that both S3 and S4 (but probably not at the same time) of OGT can be *O*-GlcNAc modified (Figure 2D). Hence, phosphorylation by GSK3β and *O*-GlcNAcylation must compete with and regulate each other at this N-terminal site of OGT.

OGT activity was next measured in the presence and absence of GSK3β to reveal whether phosphorylation by GSK3β regulates OGT activity. Indeed, OGT activity was enhanced with the presence of GSK3β phosphorylation (Figure 2E, OGT versus pOGT). To test whether phosphorylation of S3 and S4 on OGT by GSK3β is responsible for the enhanced activity, we mutated S3 and S4 to either alanine or aspartate (to mimic a constitutively phosphorylated state) before the kinase assays. Increased OGT activity by GSK3β was blocked when S3 and S4 were mutated to alanine, providing evidence that phosphorylation on these two amino acids is necessary for the effect of GSK3β on OGT. Interestingly, when S3 and S4 were mutated to aspartate, OGT activity increased slightly in the absence of GSK3β but significantly in the presence of GSK3β, suggesting that other phosphorylation sites on OGT are needed for the complete activation of OGT activity by GSK3β.

Manipulating *O*-GlcNAcylation Levels Regulates Period Length in Both Mice and *Drosophila*

Since cyclic posttranslational modifications such as phosphorylation (Chiu et al., 2011; Xu et al., 2007), acetylation (Hirayama et al., 2007), SUMOylation (Cardone et al., 2005), and poly(ADP-ribosyl)ation (Asher et al., 2010) are known to regulate clock

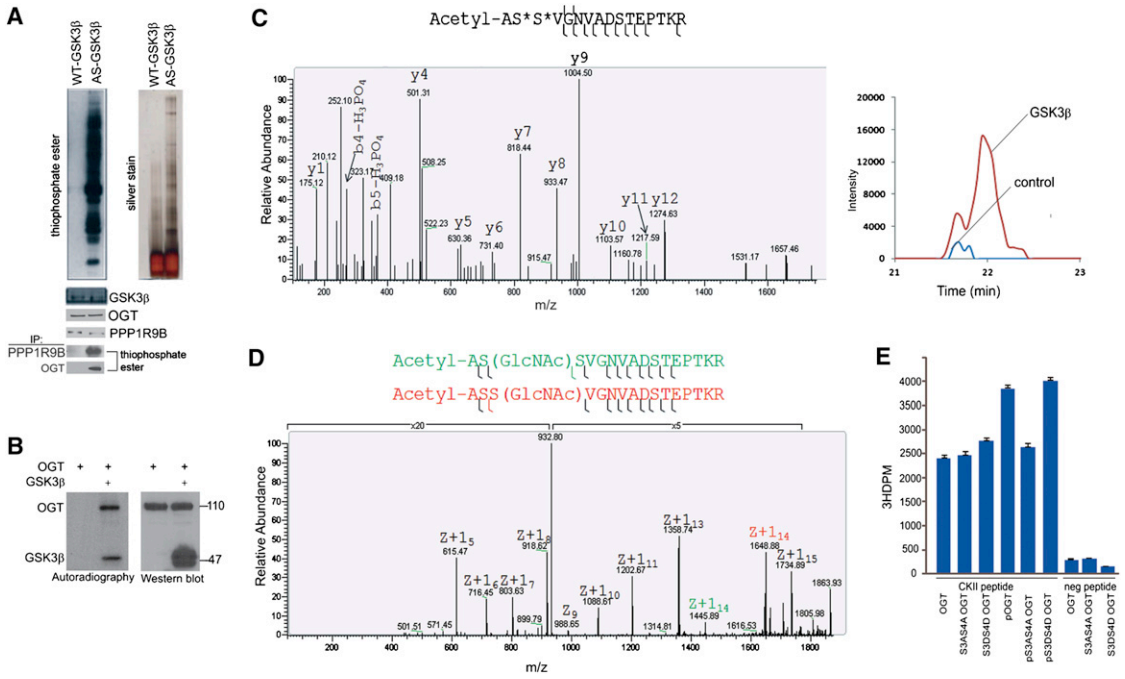

Figure 2. OGT Activity Is Regulated by GSK3β

(A) Kinase assays for mouse brain extracts from WT GSK3β or AS GSK3β were visualized by silver staining (top right panel) or by western blot against thiophosphate ester antibody (top left panel). Western blots of the same brain extracts probed with antibodies against GSK3β, OGT, and PPP1R9B (middle panels). Kinase reactions of brain extracts were immunoprecipitated by antibodies for PPP1R9B or OGT, followed by western blot against thiophosphate ester antibody (bottom panel). PPP1R9B and OGT were specifically phosphorylated by AS GSK3β, but not by WT GSK3β.

(B) In vitro phosphorylation of OGT by GSK3β in the presence of radioactive ATP (left panel). Proteins used were detected by western blotting probed with anti-OGT and anti-GSK3β antibodies (right panel).

(C) Increased phosphorylation of OGT N-terminal peptide by GSK3β. Extracted ion chromatograms of the mass-to-charge (m/z) ratio of the phosphorylated version of the tryptic peptide spanning residues 2–17 of the protein OGT shows a significantly increased level upon GSK3β treatment (right panel). CID fragmentation spectrum determines the phosphorylation to be present on either S2 or S3 of the peptide (i.e., S3 or S4 of the OGT protein) (left panel).

(D) OGT can be *O*-GlcNAc modified on S2 or S3 of the peptide. Electron-transfer dissociation (ETD) fragmentation spectrum of a singly GlcNAc-modified version of the tryptic peptide spanning residues 2–17 of the protein OGT shows a mixture spectrum, demonstrating modified versions where S2 and S3 of the peptide are both present.

(E) *O*-GlcNAcylation in vitro assay. *O*-GlcNAc transferase activity was measured using affinity-purified OGT, in the presence or absence of GSK3β, and UDP-[^{3}H] GlcNAc. OGT activity was enhanced by the presence of GSK3β (pOGT). S3 and S4 of OGT were mutated to either alanine (S3AS4A) or aspartate (S3DS4D) for the assay. CKII peptide and control peptide were used as substrates in the assay. 3HDPM: ^{3}H Disintegrations per minute. Error bars indicate the mean ± SE.

proteins for precise timing of circadian progression (Mehra et al., 2009), we investigated whether *O*-GlcNAcylation affects circadian rhythmicity. We first used primary embryonic fibroblast cells from *Per2*-luciferase mice (Yoo et al., 2005) and synchronized them with glucocorticoids followed by treatment with PUGNAc (OGA inhibitor), Alloxan (OGT inhibitor), or a pool of four siRNAs against *OGT*. Interestingly, OGT inhibitor and *OGT* siRNA (decreased *O*-GlcNAcylation) shortened, while OGA inhibitor (increased *O*-GlcNAcylation) lengthened the circadian rhythmicity of *Per2*-Luc oscillation (Figures 3A, 3B, and S3C). We then confirmed period shortening with *OGT* conditional knockout mice (Figures 3C, S3A, and S3B) to reduce *OGT* levels in vivo (knockout of *OGT* in mice causes early embryonic lethality) (Shafi et al., 2000).

Next, we asked whether *O*-GlcNAcylation is conserved as a regulatory mechanism in *Drosophila* circadian clock. We crossed *tim*(UAS)-Gal4 (Martinek et al., 2001) with UAS-RNAi*Ogt* or UAS-RNAi*Oga* to downregulate and UAS-*Ogt* or UAS-*Oga* to overexpress OGT and OGA, respectively, in *Drosophila* for behavioral analyses. *Ogt* knockdown and *Oga* overexpression both resulted in period shortening, while *Oga* knockdown and *Ogt* overexpression both led to period lengthening (Figures 3D and S3D). Together, these results suggested that *O*-GlcNAcylation is regulating the circadian clock in mice and flies and raised the possibility that clock proteins may be the direct targets of *O*-GlcNAcylation.

O-GlcNAc Modification of *Drosophila* and Mammalian Clock Components

Using *Drosophila* Schneider 2 (S2) cell culture, we identified that dClk and dPer are *O*-GlcNAcylated (Figures 4A and 4B). dClk-V5 coimmunoprecipated with Ogt and Oga (Figure 4C) from S2 cells, supporting the possibility that dClk is a target of Ogt/Oga-dependent, reversible *O*-GlcNAcylation. To show that mammalian clock proteins are also *O*-GlcNAc modified, human PER2-His and human OGT-Flag were coexpressed. PER2 was detected by *O*-GlcNAc antibody after anti-His immunoprecipitation, whereas *O*-GlcNAcylated PER2 was not detected in the

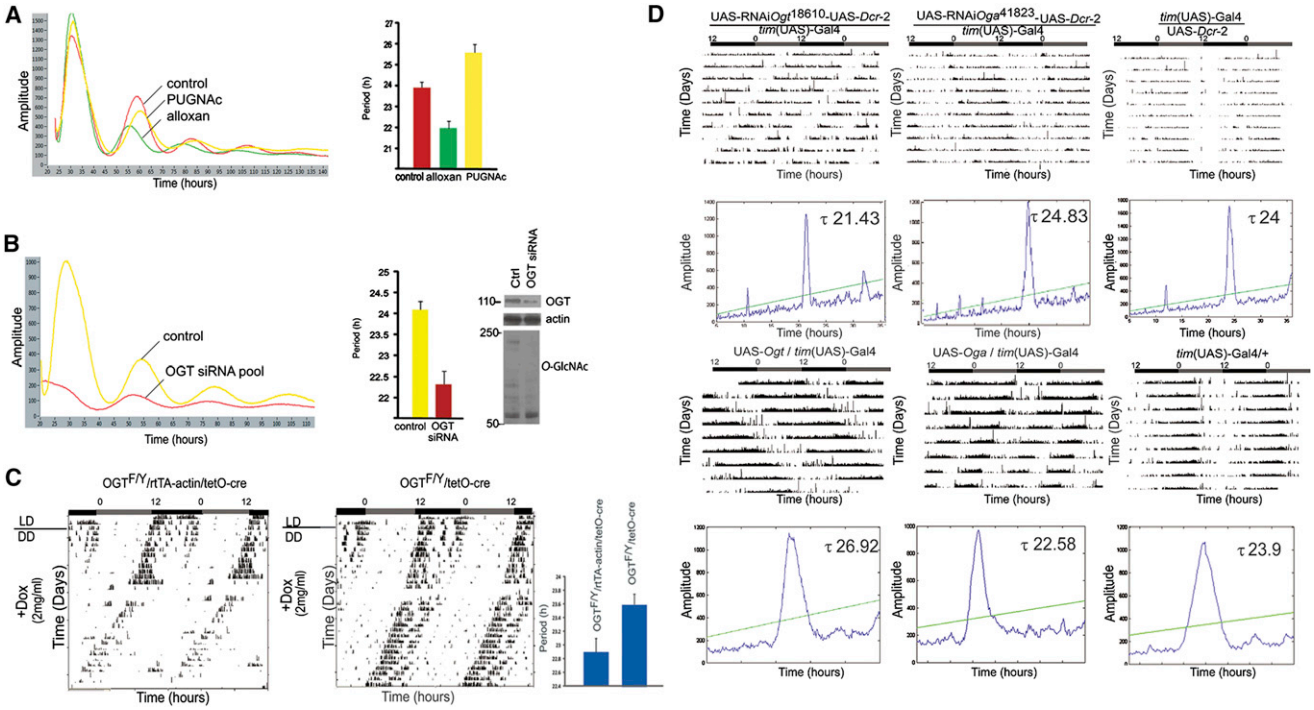

Figure 3. *O*-GlcNAcylation Levels Regulate Period Length

(A) Alloxan (1 mM; OGT inhibitor) shortens (22.2 hr ± 19 min) and PUGNAc (100 μM; OGA inhibitor) lengthens (25.6 hr ± 15 min) the circadian period of primary fibroblasts extracted from *Per2*-Luc reporter mice. For control, the periods of *Per2*-Luc fibroblasts were measured as 24.2 hr ± 21 min. Concentrations of Alloxan and PUGNAc were experimentally tested in pilot experiments (data not shown). A representative of experiments repeated in triplicate is illustrated.

(B) A pool of four *OGT* siRNAs shortens *Per2*-Luc fibroblast periods to 22.5 hr ± 20 min compared to the control siRNA pool at 24.4 hr ± 30 min. A representative of experiments repeated in triplicate is illustrated. OGT and *O*-GlcNAc levels in the control and siRNA cells were determined by western blotting shown to the right.

(C) $OGT^{F/Y}$-rtTA-actin/tetO-cre (conditional knockout) and $OGT^{F/Y}$/tetO-cre (control) mice were entrained in a 12 hr dark/12 hr light cycle. The mice were released to constant darkness before doxycycline (2 mg/ml) was supplemented into drinking water. Representative locomotor activity recordings of indicated mouse genotypes are presented. For visualization, 2 days are plotted per row. Quantifications of period length by hours are shown in the right panel. n = 8 for both mice genotypes.

(D) Representative locomotor activity recordings and periodograms of indicated fly genotypes over circadian time. For visualization, 2 days are plotted per row. On top of the panels, the subjective light (gray bar) and dark (black bar) phases are indicated. Numbers in the oscillation graphs indicate τ, the expressed period of the free-running rhythm in constant darkness, of flies with the indicated genotype. Details and quantifications are specified in Table S4. Controls for (A), (C), and (D) are shown in Figure S3. Error bars represent SEM. See also Figure S3.

presence of excess GlcNAc in the buffer, suggesting *O*-GlcNAcylation of PER2 is specific (Figure 4D). In the presence of OGA inhibitor (PUGNAc) in the lysis buffer, PER2-His was also detected as *O*-GlcNAc modified without cotransfection with OGT, further supporting that PER2 is modified by *O*-GlcNAc (Figure 4E). Immunoprecipitation was next performed with mouse liver extracts using anti-*O*-GlcNAc antibody, and western blot analysis indicated *O*-GlcNAcylation of both mouse PER2 and OGT in vivo (Figure 4F). Similarly, mouse CLOCK is likely *O*-GlcNAcylated by OGT and de-*O*-GlcNAcylated by OGA in HEK293 cells (Figure 4G). Using mouse liver extracts, OGA coimmunoprecipitated with CLOCK at circadian times CT8 and CT20 (Figure 4H), indicating that CLOCK interacts with OGA and is likely a target of OGT/OGA-dependent *O*-GlcNAcylation.

O-GlcNAcylation Modulates dClk and dPer Transcriptional Activities

To gain further insight into the effect of *O*-GlcNAcylation on dClk in circadian regulation, we employed a luciferase assay to measure dClk-dependent E-box activation of the *per* promoter in the presence of Ogt or Oga (Figure 5A) and demonstrated that de-*O*-GlcNAcylated dClk activates and *O*-GlcNAcylated dClk represses E-box-dependent *per*-luc activation more than basal dClk (i.e., without exogenous Ogt or Oga). Interestingly, the transcriptional activity of dClk when dClk and dPer are both de-*O*-GlcNAcylated is similar to the activity of dClk without dPer, and the repressive effect of dPer is further enhanced when dClk and dPer are both *O*-GlcNAcylated, implying that Ogt enhances and Oga relieves dPer-dependent *per*-luc inhibition through dClk. These results demonstrate that *O*-GlcNAc modification of dClk transcriptional activity is integral for regulation of the molecular clock.

Since *O*-GlcNAcylation modulates dClk transcriptional activity, we next measured dTim and dPer levels. When *Ogt* is overexpressed (i.e., reduced dClk transcriptional activity), both dTim and dPer levels were reduced compared to control flies, and their rhythm phases showed a subtle trend of delay in clock neurons (Figures 5B and S4B). On the other hand, *Ogt* RNAi (i.e., increased dClk transcriptional activity) resulted in increased d*Tim* and d*Per* protein (Figure 5C) and RNA levels (Figure 5D),

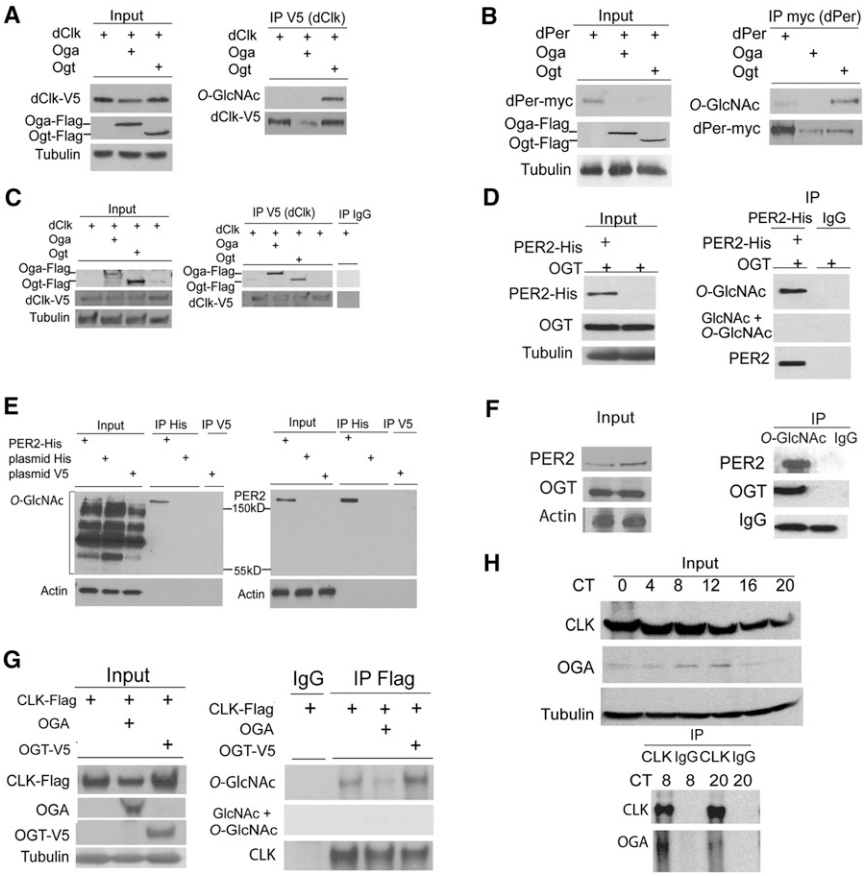

Figure 4. *O*-GlcNAcylation of Clock Proteins

(A) dClk-V5 was transfected into S2 cells alone or together with Ogt-Flag or Oga-Flag followed by dClk-V5 pull-down and *O*-GlcNAc western analysis.

(B) dPer-myc was transfected into S2 cells alone or together with Ogt-Flag or Oga-Flag followed by dPer-myc pull-down and *O*-GlcNAc western analysis.

(C) dClk-V5 was transfected into S2 cells alone or together with Ogt-Flag or Oga-Flag, and dClk-V5 pull-down was performed using V5. Western blot was performed with Flag antibody. IgG was used as negative control for pull-down.

(D) Human PER2 (PER2) is *O*-GlcNAcylated in HEK293 cells (upper panel). GlcNAc in the western buffer blocks the interaction of *O*-GlcNAc antibody with PER2, indicating that PER2 is *O*-GlcNAcylated (middle panel).

(E) hPER2-His or empty plasmids were transfected into HEK293 cells, and pull-down was performed with His or V5 antibodies. The OGA inhibitor PUGNAc was included in the lysis buffer, and western blot was probed with *O*-GlcNAc (left panel) or PER2 (right panel) antibodies. In the presence of PUGNAc, PER2 is *O*-GlcNAcylated without additional OGT (left panel). Cells transfected with empty plasmids were included as negative controls.

(F) Western analysis for immunoprecipitants using anti-*O*-GlcNAc from mouse liver extracts with anti-PER2 (mouse PER2) and anti-OGT antibodies demonstrate that PER2 is *O*-GlcNAc modified. OGT is auto-*O*-GlcNAcylated and serves as a positive control. IP with IgG was used as a negative control.

(G) mCLOCK (CLK) is *O*-GlcNAcylated by OGT and de-*O*-GlcNAcylated by OGA. CLK-Flag was transfected into HEK293 cells either alone or together with OGA or OGT-V5 followed by Flag pull-down and *O*-GlcNAc western analysis.

(H) CLOCK protein interacts with OGA in the mouse liver. CLOCK protein was immunoprecipitated from the mouse liver at CT8 and CT20. Western blot of the CLK pull-down was probed with CLK and OGA antibodies (bottom panel). Inputs are shown over the time course including CT8 and CT20 (top panel).

which were accompanied by clear advances of the phase. Taken together, these results point to the necessity for balanced OGA and OGT activities and tightly controlled levels of *O*-GlcNAc-modified clock components for proper clock function.

Competition of *O*-GlcNAcylation and Phosphorylation for the PER2 S662–S674 Region

Human PER2 S662–S674 is a critical site for regulating clock speed by serial phosphorylation of multiple residues; a serine (S662) to glycine mutation leads to hypophosphorylation of this region and causes familial advanced sleep-phase disorder (Toh et al., 2001). We hence investigated the possibility that *O*-GlcNAcylation interplays with phosphorylation at S662–S674, and tandem mass spectrometry (MS/MS) analyses were carried out to identify *O*-GlcNAc sites on PER2 focusing on this region (Figure 6A). *O*-GlcNAcylation can occur on S662, and this only occurs together with *O*-GlcNAcylation on S671 (Figure 6A), implying a potential antagonism of *O*-GlcNAcylation with phosphorylation in this region. Interestingly, *O*-GlcNAc sites found with our method concentrate in the CK1 binding domain (S566, S580, S653, S662, S668, S671, and T734) and in the C terminus (T965, S983, and T1180) of PER2 (Figure 6B). To investigate the possible interplay between phosphorylation and *O*-GlcNAcylation on PER2 S662–S674, HEK293 cells were transfected with PER2-His alone or cotransfected with either OGT or OGA, followed by immunoprecipitation with His antibody. Western blot analysis using an antibody specific for phospho-S662 PER2 revealed that phosphorylated S662 PER2 level was reduced in cells cotransfected with PER2 and OGT, while *O*-GlcNAcylation was increased on PER2, suggesting that *O*-GlcNAcylation can block S662 phosphorylation (Figure 6C). However, neither OGT nor OGA interfered with the binding of CK1 to PER2. PER2 peptides (Xu et al., 2007) containing either S662 or pS662 were then used in an *O*-GlcNAcylation assay, and pS662 peptides significantly reduced the capacity for *O*-GlcNAcylation (Figure 6D), supporting the competitive interplay between phosphorylation and *O*-GlcNAcylation at S662. Consistent with the finding for dClk and dPer transcriptional activity (Figure 5A), OGT inhibited CLK-BMAL1 transcription and further enhanced PER2 repressor activity (Figure S5). This is congruent with the previous finding that PER2-S662G is a stronger repressor than WT PER2 (Xu et al., 2007), and as expected, repressor activity of PER2-S662G is not modulated by OGT (Figure S5). Taken together, these data strongly suggest that *O*-GlcNAcylation and phosphorylation compete at S662 of PER2 to fine-tune its activity.

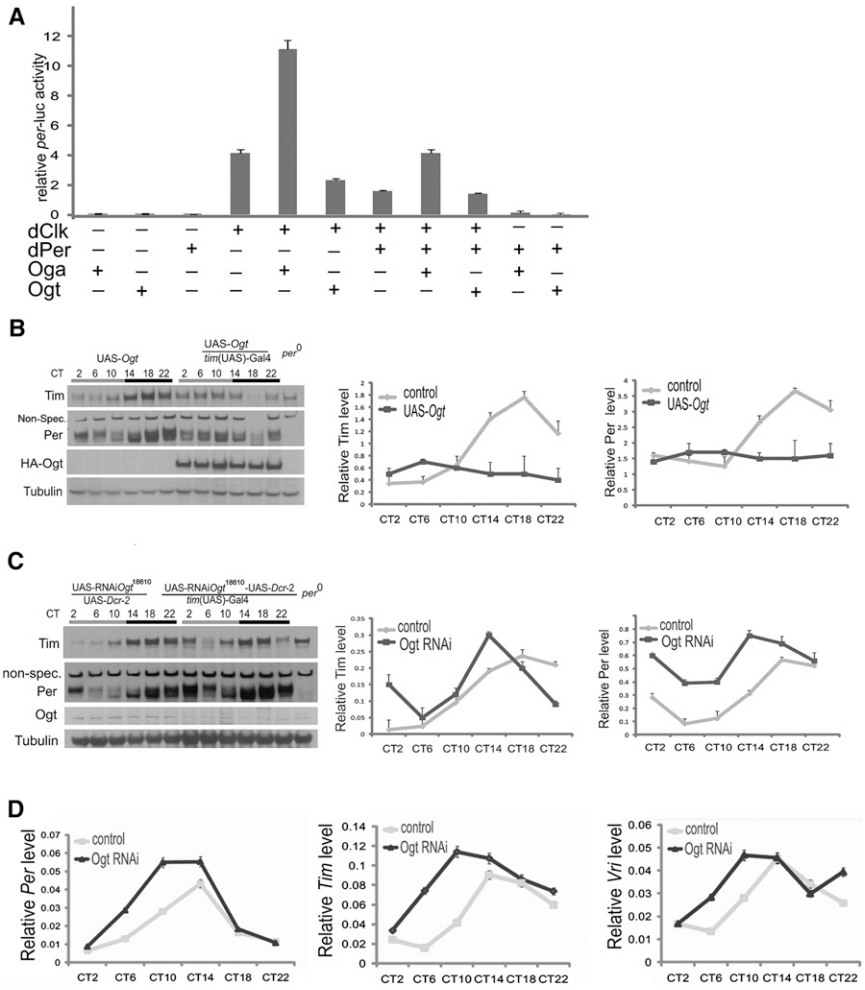

Figure 5. Functional Effects of *O*-GlcNAcylation on dClk

(A) The effects of *Oga* and *Ogt* on dClk-dependent *per*-luc activity. Luciferase assays were performed in triplicate on at least three independent occasions.

(B and C) dTim, dPer, and dOgt protein levels under *Ogt* overexpression (B) and *Ogt* RNAi (C) as illustrated by western analyses (left panels) and quantifications (right panels).

(D) Quantification of *Per*, *Tim*, and *Vri* mRNA levels from *Ogt* RNAi flies by qRT-PCR. Three independent experiments were used for each circadian time point. Error bars represent SEM. See also Figure S4.

Since *O*-GlcNAcylation is the direct readout for the hexosamine biosynthetic pathway (HBP; converting glucose to UDP-GlcNAc), a nutrient sensing pathway through glucose, we further investigated the impact of glucose on *O*-GlcNAcylation and phosphorylation of PER2 S662, S665, and S668. We employed an in vitro system with glucose levels that were established previously for this analysis (Lamia et al., 2009). In the presence of high glucose, but not low glucose, OGT was able to block the phosphorylation by CK1δ of this region (Figure 6E, right panel, lanes 3 and 4), suggesting that high glucose levels likely increase *O*-GlcNAcylation, which blocks phosphorylation of the PER2 S662–S668 region. Intriguingly, high glucose can significantly prevent phosphorylation even in the presence of OGA (Figure 6E, right panel, lane 6). Given the role of PER2 S662 phosphorylation in regulating human clock (Xu et al., 2007), these results suggest that glucose metabolism and *O*-GlcNAcylation modulate the circadian clock partially through *O*-GlcNAcylation's competition with phosphorylation in the PER2 S662 region (Figure 6F).

O-GlcNAcylation Is Regulated by Circadian Clock

Since phosphorylation and *O*-GlcNAcylation both modify serine and threonine residues, and multiple phosphorylation events are known to exhibit circadian oscillation, we set out to determine whether *O*-GlcNAc modification on clock proteins also oscillates. dClk was pulled down from the heads of yw;;dClk-V5 flies (Menet et al., 2010) at different circadian time points and then immunoblotted with *O*-GlcNAc antibody. Endogenous dClk protein underwent *O*-GlcNAc modification in a time-dependent manner peaking at ZT10 (Figures 7A and 7B), though total dClk protein levels oscillate in the opposite phase. dPer coimmunoprecipitated with dClk (Menet et al., 2010) and exhibited a similar rhythmic *O*-GlcNAc modification pattern (Figures 7A and 7B). Similarly, dClk and dPer *O*-GlcNAcylation peaked in constant conditions at CT10–CT14 (Figures S6A and S6B). In addition, like what was found for mammalian CLOCK (Figure 4G), Oga protein coimmunoprecipitated with the dClk/dPer complex in vivo (Figure S6B). These results indicate that *O*-GlcNAc modification is likely under circadian clock regulation. We next analyzed OGT and OGA protein expression levels from liver tissues of WT mice over circadian time. Expression levels of OGT (110 kDa) did not oscillate. However, OGA protein exhibited an oscillating expression pattern that peaks around CT8–CT12 (Figure 7C) (*OGA* mRNA expression also oscillates with a peak at CT2.3; http://bioinf.itmat.upenn.edu/circa). Ogt and Oga protein levels of WT fly heads showed expression patterns similar to mouse liver (Figures 7D and 7E). Therefore, while OGA protein levels (and presumably total OGA activity) oscillate in a circadian manner, OGT protein levels are constant. But OGT activity is modulated by GSK3β (Figure 2), and GSK3β activity is known to oscillate through S9 phosphorylation. This would imply that OGT activity could also oscillate. Interestingly, we found that the *O*-GlcNAc on OGT itself showed a possible oscillating modification pattern through time (Figure S6E), which supports the likelihood that OGT activity oscillates. Taken together, these data suggest that both OGT incorporation of donor sugar nucleotides to proteins and OGA removal of these sugar nucleotides occur in a circadian time-dependent manner.

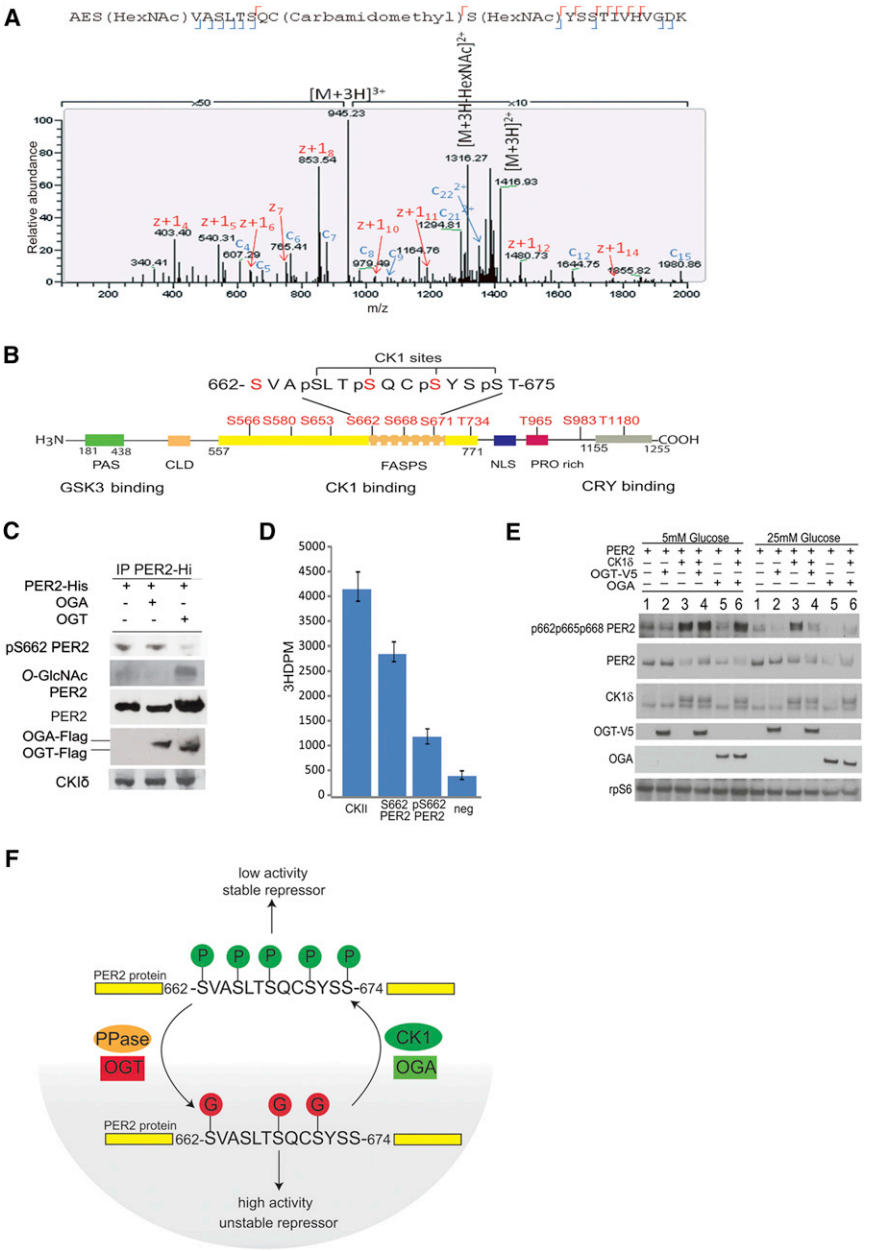

Figure 6. Competition of *O*-GlcNAcylation and Phosphorylation for Residues in the PER2 S662–S674 Region

(A) MS/MS spectrum of the doubly *O*-GlcNAc-modified PER2 S660–S682 region. Full-length human PER2 was purified using FLAG affinity tag from the HEK293 cells before being subjected to MS/MS analysis. Modified c_4 and c_5 ions localize one of the modification sites to S662, while the mass shift between unmodified z + 1_{11} and modified z + 1_{12} pinpoints the second modification site to S671.

(B) MS/MS identified *O*-GlcNAc sites S566, S580, S653, S662, S668, S671, T734, T965, S983, and T1180 (labeled in red) for PER2 in the CK1 binding domain (amino acids 557–771) and C terminus. The identified S662, S668, and S671 *O*-GlcNAc sites are also CK1 phosphorylation sites.

(C) Western blots performed with antibodies indicated on the left demonstrating that the presence of OGT inhibits PER2 S662 phosphorylation, but the presence of either OGT or OGA does not block CK1 binding to PER2.

(D) In vitro *O*-GlcNAcylation assay using affinity-purified OGT peptides and UDP-[^{3}H]GlcNAc. *O*-GlcNAcylation of pS662 PER2 peptide is significantly reduced compared to nonphosphorylated S662 PER2 peptide. CKII and Vangl1 peptides served as positive and negative controls, respectively. Error bars indicate the mean ± SE.

(E) The PER2 S662 region is regulated by both *O*-GlcNAcylation and phosphorylation. PER2 was transfected alone (lane 1) or with OGT (lane 2), CK1 (lane 3), OGT and CK1 (lane 4), OGA (lane 5), and OGA and CK1 (lane 6) in the presence of low (left panel) or high (right panel) glucose into HEK293 cells. Western blots of protein extracts from these cells were probed with antibodies indicated on the left of the panels.

(F) Proposed model for competitive regulation by *O*-GlcNAcylation and phosphorylation of the PER2 S662–S674 region. When PER2 S662–S674 is hypophosphorylated (i.e., *O*-GlcNAcylated), it is known to be a stronger repressor with lower protein stability, whereas when this region is hyperphosphorylated, it is a weaker repressor with higher stability (Xu et al., 2007). See also Figure S5.

DISCUSSION

We developed an analog-specific chemical-genetic proteomic approach to characterize the GSK3β-dependent circadian phosphoproteome and identified OGT as a GSK3β substrate. Here, we found that OGT is phosphorylated at S3 or S4 by GSK3β and that *O*-GlcNAcylation of OGT also occurs on the same or neighboring serine residues, suggesting interacting phosphorylation and *O*-GlcNAcylation events on OGT itself.

OGT is expressed constitutively, while OGA levels oscillate with a peak around CT8–CT12, and phosphorylation of OGT by GSK3β increases OGT activity. Given that GSK3β activity oscillates through circadian time, it implies that the activity of OGT oscillates. OGT activity is likely further regulated by additional modulations including auto-*O*-GlcNAcylation. Intriguingly, the *O*-GlcNAc modification patterns of OGT support a possibility for oscillating OGT activity. Moreover, OGA activity may also be regulated by other factors and posttranslational modifications. Interestingly, OGA was also identified in our GSK3β chemical-genetic screen (Table S1). Together, all these pathways contribute to the determination of *O*-GlcNAcylation oscillation patterns of clock components. Hence, it is possible that the peak of *O*-GlcNAc modification of clock proteins may not have obvious correlation with the peak of OGA expression. This intricate regulatory system is therefore multilayered and consistent with the notion that delicately modulated mechanisms are required for circadian regulation at different levels. Recently, *O*-GlcNAcylation was shown to modulate both the *Drosophila*

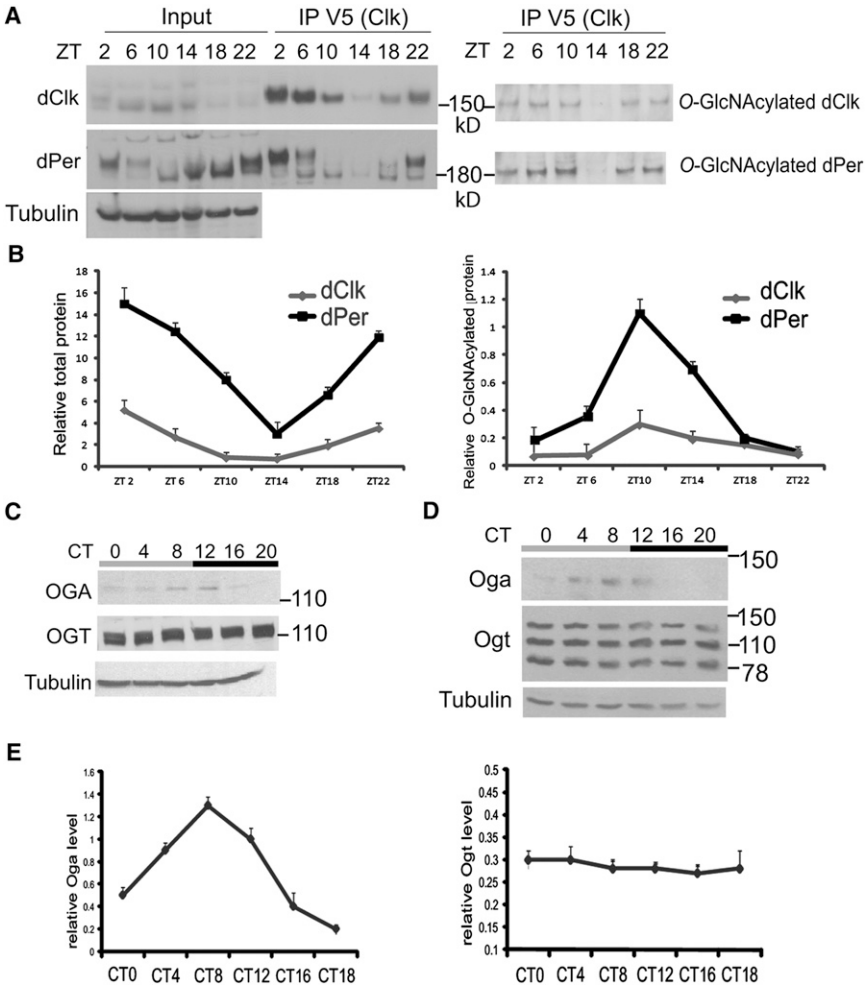

Figure 7. *O*-GlcNAcylation Is Regulated by Circadian Clock

(A) dClk was pulled down from yw;;dClk-V5 flies (one extra copy of Clk) at different zeitgeber times (ZT) prior to being immunoprecipitated by V5 antibody. Immunoprecipitated preparations were run on identical gels. Western blots of these gels were then immunoblotted by dClk, dPer, Tubulin (left panels), and *O*-GlcNAc (right panels) antibodies, separately.

(B) Quantification of immunoprecipitated proteins (left panel) and *O*-GlcNAcylated proteins normalized with immunoprecipitated protein levels (right panel).

(C) Immunoblotting indicates that OGA protein levels oscillate over 24 hr, and OGT expression levels (110 kDa band) are constant over 24 hr in extracts of mouse liver tissue.

(D) Oga shows oscillation over 24 hr, and Ogt expression is constant in protein extracts from WT fly heads.

(E) Quantification of (D). Error bars represent SEM. See also Figure S6.

Per (Kim et al., 2012) and the mammalian BMAL1 (Durgan et al., 2011) in regulating circadian clock. Though some discrepancies exist among different reports, one consistent finding is the modulation of circadian period length by the level of *O*-GlcNAcylation. In addition, OGT overexpression leading to reduction in Period protein levels was found by two independent studies (by us and the Durgan group). This modulation of PER levels by *O*-GlcNAcylation could be one of the major reasons for the observed period changes, since it has been shown that PER rhythmic abundance is the driving force for the clock oscillation (Chen et al., 2009; Yu et al., 2006). Additional work is needed to identify site-specific roles of *O*-GlcNAcylation and then their interplay with phosphorylation and other posttranslational modifications in clock proteins in order to further reveal the complex regulatory mechanisms of the circadian rhythms.

Protein *O*-GlcNAcylation has been shown to regulate transcriptional machinery (Ozcan et al., 2010). For example, the RNA polymerase (pol) II C-terminal domain is modified by both phosphorylation and *O*-GlcNAcylation in a mutually exclusive manner. It was proposed that transcriptionally inactive *O*-GlcNAcylated RNA pol II holoenzyme localizes to promoters in a poised state but can only effect transcriptional elongation when the C-terminal domain *O*-GlcNAc is removed and becomes hyperphosphorylated upon gene activation (Comer and Hart, 2001). It is possible that a similar mechanism is utilized to fine-tune the activity of Clock transcriptional function. Another possibility is that the balance between *O*-GlcNAcylation and phosphorylation of Clock modulates interactions between Clock and its binding partners (such as repressors) in a similar manner to what has been shown for Myc (Kamemura et al., 2002). Our finding that *O*-GlcNAcylation of the PER2 S662 regulatory region blocks CK1-dependent PER2 phosphorylation also supports the latter hypothesis. The phospho-*O*-GlcNAc switch therefore provides a possible mechanism for tight control of the molecular clock in order to maintain precise daily rhythms. Many questions remain, such as how do *O*-GlcNAcylation and other posttranslational modifications (in addition to phosphorylation) synergistically regulate the intricate circadian clock? CLOCK has acetyltransferase activity and regulates chromatin remodeling through the acetylation of BMAL1 (Hirayama et al., 2007), and Ogt has been identified as a repressor from the polycomb complex (Gambetta et al., 2009; Myers et al., 2011). Thus, the fact that clock proteins are modified by OGT/OGA connects the HBP and epigenetics (Polycomb as a protein complex for chromatin modulation) to the circadian core clock loop. Since protein *O*-GlcNAcylation is regulated principally by substrate UDP-GlcNAc availability, and HBP (a nutrient sensor) flux is known to parallel substrate (glucose) availability, our results showing that high glucose blocks CK1-dependent PER2 phosphorylation (Figure 6E) raise the intriguing possibility that the HBP and *O*-GlcNAc turnover represent a glucose-dependent mechanism for regulating circadian clocks and support the connection for metabolic pathways and molecular clock. Interestingly, circadian misalignment was shown to increase blood sugar concentrations in human (Buxton

et al., 2012; Scheer et al., 2009), indicating that the timing of nutrient intake needs to be correlated with the timing of circadian expression of genes responsible for metabolism. Our finding that glucose levels through *O*-GlcNAcylation can modulate circadian clock protein further provides evidence that nutrient intake (and its timing) and circadian clock have a closely maintained cooperative relationship. In total, our data represent a further step toward a greater understanding of the complex mechanisms that control our bodily circadian functions in a highly coordinated manner.

EXPERIMENTAL PROCEDURES

Plasmid Constructs

See Supplemental Experimental Procedures.

Kinase Assay

Nonradioactive

Glutathione S-transferase (GST) fusion of either WT GSK3β or AS GSK3β protein was expressed in *E.coli* and purified by Glutathione Sepharose 4B (GE Healthcare) (Kosuga et al., 2005). The GST tag was then removed by PreScission Protease digestion (GE Healthcare). AS GSK3β kinase activity was comparable to commercial GSK3β kinase activity (New England Biolabs). For kinase assay, 100 nM recombinant WT GSK3β or AS GSK3β was used (Allen et al., 2007). Kinase assay buffer contains 20 mM HEPES (pH 7.5), 10 mM $MgCl_2$, 0.01 mM DTT, 0.2 mM ATPγS (or ATPγS analogs), 1 mM GTP, and 1 mM ATP. Either 2 μg MBP or 5 μg GSK3β was used as AS GSK3β substrate. Reactions were incubated for 10 min at room temperature (RT) and terminated by 2.5 mM EDTA. Alkylating agent, 2 mM p-nitrobenzyl-mesylate (PNBM), in dimethyl sulfoxide (DMSO) was added, and reactions were incubated for 1.5 hr at room temperature. Laemmli buffer was added, and the samples were analyzed by western blotting.

Radioactive

Recombinant human OGT protein (350 ng; OriGene) was phosphorylated by 1000 U GSK3β (New England Biolabs) for 15 min at 30°C in 1× GSK3 buffer (New England Biolabs) and supplemented with 0.5 μl ^{32}P-labeled ATP (3,000 Ci/mmol) and 200 μM of cold ATP. For negative control reactions, OGT was incubated without GSK3β. Proteins were separated by 4%–12% Tris-HCl gels (Bio-Rad Laboratories) and transferred to nitrocellulose membrane for autoradiography or western blot.

Assay for OGT Activity

Recombinant human OGT-V5, S3AS4A Ogt-V5, or S3DS4D Ogt-V5 (100 ng) was purified from HEK293 cells. OGT was eluted with V5 peptide from the agarose beads and was phosphorylated by GSK3β (New England Biolabs) for 1 hr at RT in the presence of ATP in 1× GSK3β buffer with 200 μM of cold ATP. For the unphosphorylated OGT, the reactions were carried out without ATP. For the OGT activity assay, pOGT and OGT were incubated with 500 μM of CKII peptide (^{340}PGGSTPVSSANMM^{352}) in the presence of 0.02 μCi of UDP-[^{3}H]GlcNAc (NEN Life Science Products) in 25 mM 5′ AMP, 500 mM sodium cacodylate (pH 6.0), and 10 mM 1-amino-GlcNAc (Sigma-Aldrich). Reactions were incubated for 30 min at RT and stopped by 50 mM formic acid. Reactions were purified with Sep-Pak C18 Vac cartridges (Waters), peptides were eluted by methanol, and ^{3}H incorporation to the peptide was measured by scintillation counter. Reactions were performed in triplicates. Phospho-662 PER2 and PER2 peptides were described previously (Xu et al., 2007). Vangl1 peptide ^{517}RLQSETSV^{524} was used as the negative control.

Cell Culture

For transient protein expression, HEK293 cells were transfected with the following plasmids: h*PER2*-His, hS662G *PER2*-His, h*PER2*-Flag, m*CLOCK*-Flag, m*BMAL1*, h*OGT*-V5, h*OGA*-Flag, or*CK1δ*-myc. FuGENE HD transection reagent was used according to the manufacturer's protocol (Roche). TAP buffer supplemented with 100 μM PUGNAc was used for immunoprecipitation (IP) (Angers et al., 2006). pGL3-TAT (Meijsing et al., 2009) and per2-luc plasmid (Kaasik and Lee, 2004) were used for luciferase assay. Anti-Flag M2 Affinity Gel (Sigma-Aldrich) or His antibody (Sigma-Aldrich) was used for pull-down.

Mouse Models

All experiments with mice were conducted according to protocols approved by the Institutional Animal Care and Use Committee at the University of California, San Francisco. GSK3β$^{AS/AS}$ homozygous knockin mice were obtained from Taconic. To specifically inhibit GSK3β$^{AS/AS}$ with AS kinase inhibitors such as 1-Na-PP1, GSK3β$^{AS/AS}$ knockin mice in wheel-running cages were entrained in a light/dark cycle (12 hr light/12 hr dark) for 1 week. Mice were then released into constant darkness for 2 weeks. Intraperitoneal injection of 1 mM 1-Na-PP1 (100 μM per 25 g body weight) was given at CT12 every day for a week beginning after 1 week in constant darkness. Ogt$^{tm1Gwh/Y}$ mice were a gift from Dr. J. Marth (Shafi et al., 2000). TetO-cre and actin rtTA mice were obtained from the Jackson Laboratory (Perl et al., 2002; Sarin et al., 2005). Five OGT$^{F/Y}$/tetO-cre/and five OGT$^{F/Y}$-rtTA-actin/tetO-cre mice in wheel-running cages were entrained in a light/dark cycle (12 hr light/12 hr dark) for 1 week. Mice were then released into constant darkness for 3 weeks, and doxycycline hydrochloride (Sigma-Aldrich) was supplied in the drinking water at a concentration of 2 mg/ml. The doxycyline-containing water was renewed every 3 days. Wheel-running activity was recorded and analyzed by ClockLab.

Fly Cell Culture, Transgenic Fly, and Locomotor Behavior Analysis

Drosophila luciferase assay was carried out as described previously (Kivimäe et al., 2008). Knockdown and overexpression of Ogt (CG10392) and Oga (CG5871) was performed using *Drosophila*. For knockdown, UAS-RNAi lines of Ogt (18610, 18611) and Oga (41823, 41822) were obtained from the Vienna *Drosophila* RNAi Center (Dietzl et al., 2007). To enhance the knockdown effect, transgenic flies were crossed with UAS-Dicer2. The Tim-UAS-GAL4 driver was used to knockdown or overexpress Ogt and Oga (Blau and Young, 1999). UAS-HA-Ogt (or UAS-Ogt) and UAS-HA-Oga (or UAS-Oga) flies were generated to overexpress Ogt and Oga using the GAL4 system (Genetic Services, Inc). Analysis of locomotor activity of individually housed male flies (or virgin females) was performed in constant darkness at 25°C using the *Drosophila* Activity Monitoring System (TriKinetics). Per^0 flies were obtained from the *Drosophila* Stock Center (Bloomington, IN), and yw;;Clk-V5 flies were obtained from a previous report (Menet et al., 2010).

LumiCycle Analysis

Primary fibroblasts from *Per2*-luc mice (Yoo et al., 2004) at E13–E14 were extracted, cultured, and treated with 0.1 μM dexamethasone (Sigma-Aldrich) to reset circadian clock. PUGNAc (Toronto Research Chemicals, Inc.) was used to inhibit OGA, and Alloxan (Sigma-Aldrich) was used to inhibit OGT. Pools of four siRNAs of *OGT* were used and delivered with Accell siRNA reagent to primary *Per2*-luc fibroblasts (Dharmacon). Luciferase reporter activity was measured in the LumiCycle (Actimetrics).

Statistical Analysis

Significant differences were determined by applying one-tailed or two-tailed Student's t tests depending on the sample types. Wheel-running activity was compared between groups using repeated standard t tests for pairwise comparisons. Quantitative RT-PCR (qRT-PCR) results were analyzed by Student's t test. Error bars indicate the mean ± SE.

SUPPLEMENTAL INFORMATION

Supplemental Information includes seven figures, four tables, and Supplemental Experimental Procedures and can be found with this article online at http://dx.doi.org/10.1016/j.cmet.2012.12.017.

ACKNOWLEDGMENTS

The authors are grateful to Dr. Chao Zhang for providing 1-Na-PP1; Dr. Michael Rosbash for yw;;Clk-V5 flies; Dr. Michael W. Young for *Per*, *per-luc*, and *Tim* constructs; Dr. Paul Hardin for dClk antibody; Dr. Amita Sehgal for dPer and dTim antibodies; Dr. Randal S. Tibbetts for p662p665p668-PER2 antibody; Dr. Ravi Allada for the Clock-V5 construct; and Dr. Shu-Ting Lin for assistance in figure preparation. This work was supported by NIH grants

GM079180, MH074924, and HL059596 to L.J.P. and Y.-H.F., GM103481 and RR015804 to A.L.B., EB001987 to K.M.S., the Sandler Neurogenetics fund to Y.-H.F. and L.J.P., and a fellowship from the Damon Runyon Cancer Research Foundation to K.K. K.M.S. and L.J.P. are investigators of the Howard Hughes Medical Institute.

Received: May 7, 2012
Revised: October 2, 2012
Accepted: December 6, 2012
Published: February 5, 2013

REFERENCES

Abe, M., Herzog, E.D., and Block, G.D. (2000). Lithium lengthens the circadian period of individual suprachiasmatic nucleus neurons. Neuroreport *11*, 3261–3264.

Allen, J.J., Lazerwith, S.E., and Shokat, K.M. (2005). Bio-orthogonal affinity purification of direct kinase substrates. J. Am. Chem. Soc. *127*, 5288–5289.

Allen, J.J., Li, M., Brinkworth, C.S., Paulson, J.L., Wang, D., Hübner, A., Chou, W.H., Davis, R.J., Burlingame, A.L., Messing, R.O., et al. (2007). A semisynthetic epitope for kinase substrates. Nat. Methods *4*, 511–516.

Angers, S., Thorpe, C.J., Biechele, T.L., Goldenberg, S.J., Zheng, N., MacCoss, M.J., and Moon, R.T. (2006). The KLHL12-Cullin-3 ubiquitin ligase negatively regulates the Wnt-beta-catenin pathway by targeting Dishevelled for degradation. Nat. Cell Biol. *8*, 348–357.

Asher, G., Reinke, H., Altmeyer, M., Gutierrez-Arcelus, M., Hottiger, M.O., and Schibler, U. (2010). Poly(ADP-ribose) polymerase 1 participates in the phase entrainment of circadian clocks to feeding. Cell *142*, 943–953.

Bass, J., and Takahashi, J.S. (2010). Circadian integration of metabolism and energetics. Science *330*, 1349–1354.

Bishop, A.C., Ubersax, J.A., Petsch, D.T., Matheos, D.P., Gray, N.S., Blethrow, J., Shimizu, E., Tsien, J.Z., Schultz, P.G., Rose, M.D., et al. (2000). A chemical switch for inhibitor-sensitive alleles of any protein kinase. Nature *407*, 395–401.

Blau, J., and Young, M.W. (1999). Cycling vrille expression is required for a functional Drosophila clock. Cell *99*, 661–671.

Buxton, O.M., Cain, S.W., O'Connor, S.P., Porter, J.H., Duffy, J.F., Wang, W., Czeisler, C.A., and Shea, S.A. (2012). Adverse metabolic consequences in humans of prolonged sleep restriction combined with circadian disruption. Sci. Transl. Med. *4*, 29ra43.

Cardone, L., Hirayama, J., Giordano, F., Tamaru, T., Palvimo, J.J., and Sassone-Corsi, P. (2005). Circadian clock control by SUMOylation of BMAL1. Science *309*, 1390–1394.

Chen, R., Schirmer, A., Lee, Y., Lee, H., Kumar, V., Yoo, S.H., Takahashi, J.S., and Lee, C. (2009). Rhythmic PER abundance defines a critical nodal point for negative feedback within the circadian clock mechanism. Mol. Cell *36*, 417–430.

Chiu, J.C., Ko, H.W., and Edery, I. (2011). NEMO/NLK phosphorylates PERIOD to initiate a time-delay phosphorylation circuit that sets circadian clock speed. Cell *145*, 357–370.

Climent, J., Perez-Losada, J., Quigley, D.A., Kim, I.J., Delrosario, R., Jen, K.Y., Bosch, A., Lluch, A., Mao, J.H., and Balmain, A. (2010). Deletion of the PER3 gene on chromosome 1p36 in recurrent ER-positive breast cancer. J. Clin. Oncol. *28*, 3770–3778.

Cohen, P., and Frame, S. (2001). The renaissance of GSK3. Nat. Rev. Mol. Cell Biol. *2*, 769–776.

Comer, F.I., and Hart, G.W. (2001). Reciprocity between O-GlcNAc and O-phosphate on the carboxyl terminal domain of RNA polymerase II. Biochemistry *40*, 7845–7852.

Dietzl, G., Chen, D., Schnorrer, F., Su, K.C., Barinova, Y., Fellner, M., Gasser, B., Kinsey, K., Oppel, S., Scheiblauer, S., et al. (2007). A genome-wide transgenic RNAi library for conditional gene inactivation in Drosophila. Nature *448*, 151–156.

Duez, H., and Staels, B. (2008). Rev-erb alpha gives a time cue to metabolism. FEBS Lett. *582*, 19–25.

Duez, H., and Staels, B. (2010). Nuclear receptors linking circadian rhythms and cardiometabolic control. Arterioscler. Thromb. Vasc. Biol. *30*, 1529–1534.

Durgan, D.J., Pat, B.M., Laczy, B., Bradley, J.A., Tsai, J.Y., Grenett, M.H., Ratcliffe, W.F., Brewer, R.A., Nagendran, J., Villegas-Montoya, C., et al. (2011). O-GlcNAcylation, novel post-translational modification linking myocardial metabolism and cardiomyocyte circadian clock. J. Biol. Chem. *286*, 44606–44619.

Gambetta, M.C., Oktaba, K., and Müller, J. (2009). Essential role of the glycosyltransferase sxc/Ogt in polycomb repression. Science *325*, 93–96.

Hart, G.W., Slawson, C., Ramirez-Correa, G., and Lagerlof, O. (2011). Cross talk between O-GlcNAcylation and phosphorylation: roles in signaling, transcription, and chronic disease. Annu. Rev. Biochem. *80*, 825–858.

Hirayama, J., Sahar, S., Grimaldi, B., Tamaru, T., Takamatsu, K., Nakahata, Y., and Sassone-Corsi, P. (2007). CLOCK-mediated acetylation of BMAL1 controls circadian function. Nature *450*, 1086–1090.

Hirota, T., Lewis, W.G., Liu, A.C., Lee, J.W., Schultz, P.G., and Kay, S.A. (2008). A chemical biology approach reveals period shortening of the mammalian circadian clock by specific inhibition of GSK-3beta. Proc. Natl. Acad. Sci. USA *105*, 20746–20751.

Iitaka, C., Miyazaki, K., Akaike, T., and Ishida, N. (2005). A role for glycogen synthase kinase-3beta in the mammalian circadian clock. J. Biol. Chem. *280*, 29397–29402.

Kaasik, K., and Lee, C.C. (2004). Reciprocal regulation of haem biosynthesis and the circadian clock in mammals. Nature *430*, 467–471.

Kamemura, K., Hayes, B.K., Comer, F.I., and Hart, G.W. (2002). Dynamic interplay between O-glycosylation and O-phosphorylation of nucleocytoplasmic proteins: alternative glycosylation/phosphorylation of THR-58, a known mutational hot spot of c-Myc in lymphomas, is regulated by mitogens. J. Biol. Chem. *277*, 19229–19235.

Kategaya, L.S., Hilliard, A., Zhang, L., Asara, J.M., Ptáček, L.J., and Fu, Y.H. (2012). Casein kinase 1 proteomics reveal prohibitin 2 function in molecular clock. PLoS ONE *7*, e31987.

Kim, E.Y., Jeong, E.H., Park, S., Jeong, H.J., Edery, I., and Cho, J.W. (2012). A role for O-GlcNAcylation in setting circadian clock speed. Genes Dev. *26*, 490–502.

Kivimäe, S., Saez, L., and Young, M.W. (2008). Activating PER repressor through a DBT-directed phosphorylation switch. PLoS Biol. *6*, e183.

Kosuga, S., Tashiro, E., Kajioka, T., Ueki, M., Shimizu, Y., and Imoto, M. (2005). GSK-3beta directly phosphorylates and activates MARK2/PAR-1. J. Biol. Chem. *280*, 42715–42722.

Lamia, K.A., Sachdeva, U.M., DiTacchio, L., Williams, E.C., Alvarez, J.G., Egan, D.F., Vasquez, D.S., Juguilon, H., Panda, S., Shaw, R.J., et al. (2009). AMPK regulates the circadian clock by cryptochrome phosphorylation and degradation. Science *326*, 437–440.

Lubas, W.A., and Hanover, J.A. (2000). Functional expression of O-linked GlcNAc transferase. Domain structure and substrate specificity. J. Biol. Chem. *275*, 10983–10988.

Martinek, S., Inonog, S., Manoukian, A.S., and Young, M.W. (2001). A role for the segment polarity gene shaggy/GSK-3 in the Drosophila circadian clock. Cell *105*, 769–779.

Mehra, A., Baker, C.L., Loros, J.J., and Dunlap, J.C. (2009). Post-translational modifications in circadian rhythms. Trends Biochem. Sci. *34*, 483–490.

Meijsing, S.H., Pufall, M.A., So, A.Y., Bates, D.L., Chen, L., and Yamamoto, K.R. (2009). DNA binding site sequence directs glucocorticoid receptor structure and activity. Science *324*, 407–410.

Menet, J.S., Abruzzi, K.C., Desrochers, J., Rodriguez, J., and Rosbash, M. (2010). Dynamic PER repression mechanisms in the Drosophila circadian clock: from on-DNA to off-DNA. Genes Dev. *24*, 358–367.

Myers, S.A., Panning, B., and Burlingame, A.L. (2011). Polycomb repressive complex 2 is necessary for the normal site-specific O-GlcNAc distribution in mouse embryonic stem cells. Proc. Natl. Acad. Sci. USA *108*, 9490–9495.

O'Brien, W.T., and Klein, P.S. (2009). Validating GSK3 as an in vivo target of lithium action. Biochem. Soc. Trans. *37*, 1133–1138.

Ozcan, S., Andrali, S.S., and Cantrell, J.E. (2010). Modulation of transcription factor function by O-GlcNAc modification. Biochim. Biophys. Acta *1799*, 353–364.

Perl, A.K., Wert, S.E., Nagy, A., Lobe, C.G., and Whitsett, J.A. (2002). Early restriction of peripheral and proximal cell lineages during formation of the lung. Proc. Natl. Acad. Sci. USA *99*, 10482–10487.

Rayasam, G.V., Tulasi, V.K., Sodhi, R., Davis, J.A., and Ray, A. (2009). Glycogen synthase kinase 3: more than a namesake. Br. J. Pharmacol. *156*, 885–898.

Sarin, K.Y., Cheung, P., Gilison, D., Lee, E., Tennen, R.I., Wang, E., Artandi, M.K., Oro, A.E., and Artandi, S.E. (2005). Conditional telomerase induction causes proliferation of hair follicle stem cells. Nature *436*, 1048–1052.

Scheer, F.A., Hilton, M.F., Mantzoros, C.S., and Shea, S.A. (2009). Adverse metabolic and cardiovascular consequences of circadian misalignment. Proc. Natl. Acad. Sci. USA *106*, 4453–4458.

Sekine, O., Love, D.C., Rubenstein, D.S., and Hanover, J.A. (2010). Blocking O-linked GlcNAc cycling in Drosophila insulin-producing cells perturbs glucose-insulin homeostasis. J. Biol. Chem. *285*, 38684–38691.

Shafi, R., Iyer, S.P., Ellies, L.G., O'Donnell, N., Marek, K.W., Chui, D., Hart, G.W., and Marth, J.D. (2000). The O-GlcNAc transferase gene resides on the X chromosome and is essential for embryonic stem cell viability and mouse ontogeny. Proc. Natl. Acad. Sci. USA *97*, 5735–5739.

Toh, K.L., Jones, C.R., He, Y., Eide, E.J., Hinz, W.A., Virshup, D.M., Ptácek, L.J., and Fu, Y.H. (2001). An hPer2 phosphorylation site mutation in familial advanced sleep phase syndrome. Science *291*, 1040–1043.

Torres, C.R., and Hart, G.W. (1984). Topography and polypeptide distribution of terminal N-acetylglucosamine residues on the surfaces of intact lymphocytes. Evidence for O-linked GlcNAc. J. Biol. Chem. *259*, 3308–3317.

Wulff, K., Gatti, S., Wettstein, J.G., and Foster, R.G. (2010). Sleep and circadian rhythm disruption in psychiatric and neurodegenerative disease. Nat. Rev. Neurosci. *11*, 589–599.

Xu, Y., Toh, K.L., Jones, C.R., Shin, J.Y., Fu, Y.H., and Ptácek, L.J. (2007). Modeling of a human circadian mutation yields insights into clock regulation by PER2. Cell *128*, 59–70.

Yoo, S.H., Yamazaki, S., Lowrey, P.L., Shimomura, K., Ko, C.H., Buhr, E.D., Siepka, S.M., Hong, H.K., Oh, W.J., Yoo, O.J., et al. (2004). PERIOD2: LUCIFERASE real-time reporting of circadian dynamics reveals persistent circadian oscillations in mouse peripheral tissues. Proc. Natl. Acad. Sci. USA *101*, 5339–5346.

Yoo, S.H., Ko, C.H., Lowrey, P.L., Buhr, E.D., Song, E.J., Chang, S., Yoo, O.J., Yamazaki, S., Lee, C., and Takahashi, J.S. (2005). A noncanonical E-box enhancer drives mouse Period2 circadian oscillations in vivo. Proc. Natl. Acad. Sci. USA *102*, 2608–2613.

Yu, W., Zheng, H., Houl, J.H., Dauwalder, B., and Hardin, P.E. (2006). PER-dependent rhythms in CLK phosphorylation and E-box binding regulate circadian transcription. Genes Dev. *20*, 723–733.

Cell Metabolism, Volume *17*

Supplemental Information

Glucose Sensor *O*-GlcNAcylation Coordinates with Phosphorylation to Regulate Circadian Clock

Krista Kaasik, Saul Kivimäe, Jasmina J. Allen, Robert J. Chalkley, Yong Huang, Kristin Baer, Holger Kissel, Alma L. Burlingame, Kevan M. Shokat, Louis J. Ptáček, and Ying-Hui Fu

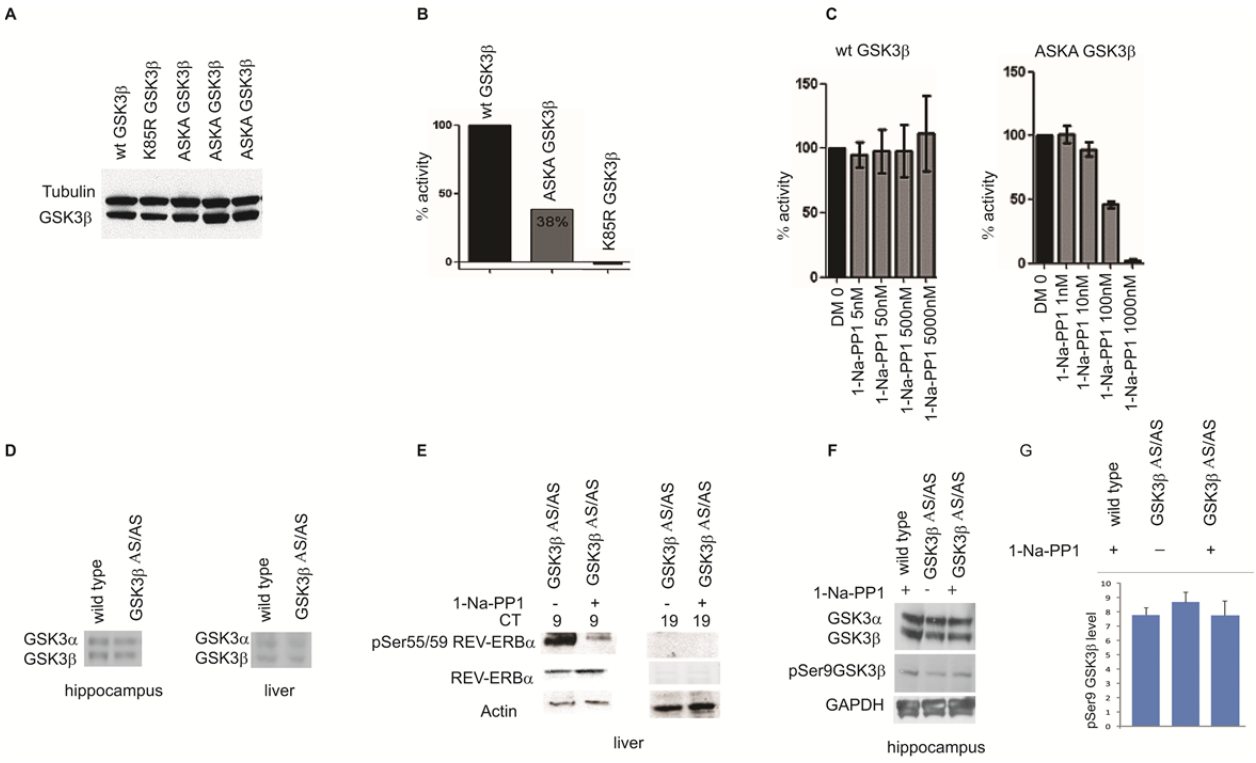

Figure S1. Characterization of ASKA GSK3β, Related to Figure 1

(A) GSK3β expression levels for WT and mutant GSK3β. V5 tagged WT GSK3β and ASKA GSK3β (Analog-Specific Kinase Allele, named by Taconic Artemis) were expressed in HEK293 cells and expression levels were probed with anti-V5 antibody. Expression levels of ASKA GSK3β are comparable to WT GSK3β. **(B)** Activity of ASKA GSK3β. HEK293 cells were transfected with WT GSK3β, ASKA GSK3β and K85R GSK3β (kinase dead) constructs. Kinase activities were determined on anti-V5 immunoprecipitates (12,5-25 ug of lysate, n=4) in an *in vitro* kinase assay using a continuous fluorescent kinase assay (Omnia from Invitrogen, peptide S/T 13). ATP concentration was 1 mM. **(C)** Inhibition of ASKA GSK3β by inhibitor 1-Na-PP1. Kinase activities were determined on anti-V5 immunoprecipitates (25 ug of lysate) in an *in vitro* kinase assay using a continuous fluorescent kinas assay (Omnia from Invitrogen, peptide S/T 13, 20 uM ATP, n=3. 1-Na-PP1 concentration is indicated. (**D**) GSK3β expression level is similar in WT and mutant GSK3β $^{AS/AS}$ mice for both hippocampus and liver tissues. GSK3α is used for the loading control. **(E)** pSer55/59 Rev-erbα is reduced after **1**-Na-PP1 inhibition in liver tissue at CT9 (left panel) suggesting the inhibition of AS-GSK3β in GSK3β $^{AS/AS}$ mice *in vivo*. At CT19 Rev-erbα and pSer55/59 Rev-erbα is not present (right panel). **(F)** GSK3β $^{AS/AS}$ with or without 1-Na-PP1 treatment in hippocampus tissue blotted with pSer9 GSK3β antibody. Expression level of pSer9 GSK3β is similar before and after 1-Na-PP1 inhibition. (G) Quantification of (F), pSer9 GSK3β normalized to GSK3β (n=6, 2 each genotype), $p<0.05$. Error bars represent SEM.

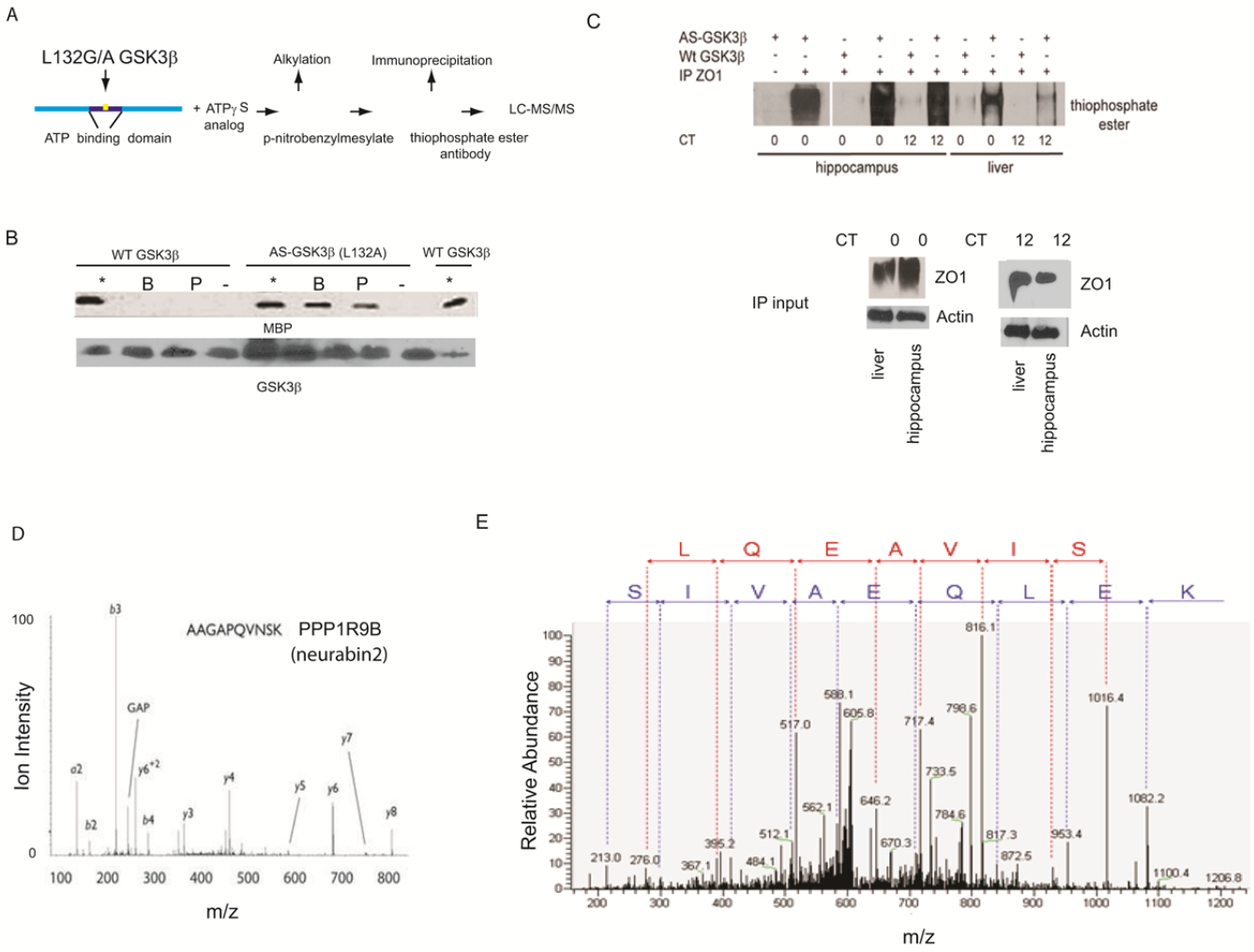

Figure S2. Chemical Proteomic Approach, Related to Figure 1

(A) Method scheme: AS-kinase (L132A GSK3β) reactions with ATPγS and ATPγS derivatives are alkylated with p-nitrophenzylmesylate, which creates an epitope for thiophosphate ester-specific antibody. Potential substrates are then immunoprecipitated with a thiophosphate ester-specific antibody, and sequenced by LC-MS/MS. (B) WT-GSK3β catalyzes γ-phosphate transfer with ATPγS but not ATPγS analogs (N6-benzyl or N6-phenethyl ATPγS) while AS-GSK3β (L132A) incorporates ATPγS analogs as well as ATPγS. See also Fig. 1 in text where AS-GSK3β (L132G) prefers ATPγS analogs over ATPγS (Figure 1C). Kinase reactions utilized myelin basic protein (MBP) as a substrate. *:ATPγS, B:N6-benzyl ATPγS, P:N6-phenethyl ATPγS, -:no nucleotides. GSK3β (last lane) from New England Biolabs was included as a positive control. Lower panel: total GSK3β visualized by Ponceau S staining. (C) GSK3β substrate ZO1 was immunoprecipitated at indicated circadian times from liver and hippocampal tissues and phosphorylated by WT GSK3β or AS-GSK3β. Western blot was probed with thiophosphate-ester specific antibody. IP inputs of ZO1 are shown at lower panel. (D, E) Examples of MS/MS for PPP1R9B and OGT.

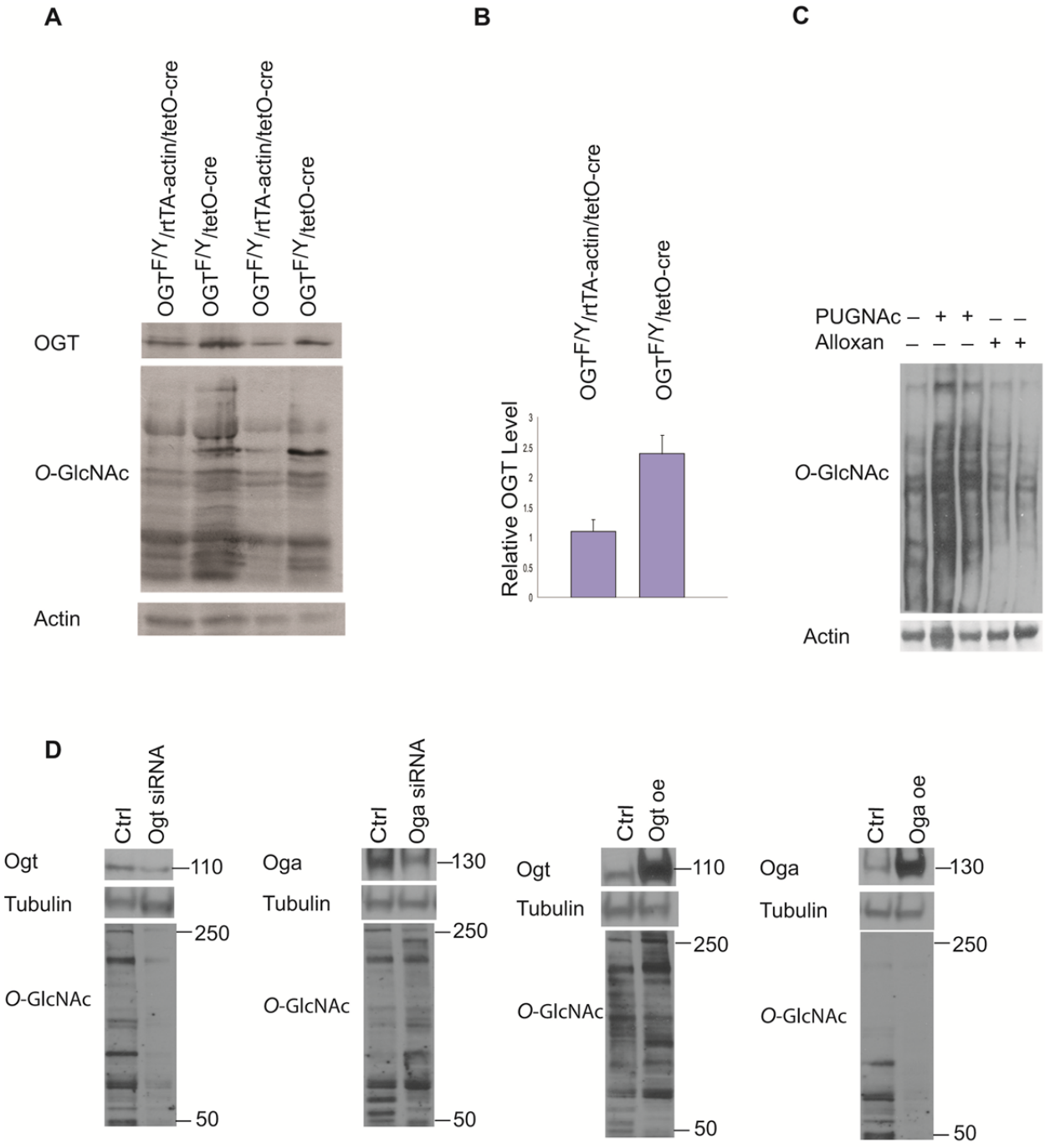

Figure S3. Confirmation of Altered OGA and OGT Protein Levels under Overexpression or Knockdown Conditions, Related to Figure 3

(A) OGT, *O*-GlcNAc and Actin levels in liver tissues from 4 independent mice with indicated genotypes measured by Western blotting. (B) Quantification of OGT levels in (A). Error bars represent SEM. (C) *O*-GlcNAc levels from *Per2*-Luc fibroblasts treated with PUGNAc 100(uM) or Alloxan (1mM) for 24 hours. (D) Western blots of fly head extracts obtained from flies used for circadian behavior analyses shown in Figure 3D. Antibodies used are indicated on the left of each panel. From left to right, protein lysates of fly heads of Ogt knockdown (siRNA), Oga knockdown (siRNA), Ogt over-expression (oe), and Oga over-expression (oe). Tubulin blotting was used as loading control. OGT and OGA levels reflect the expected changes.

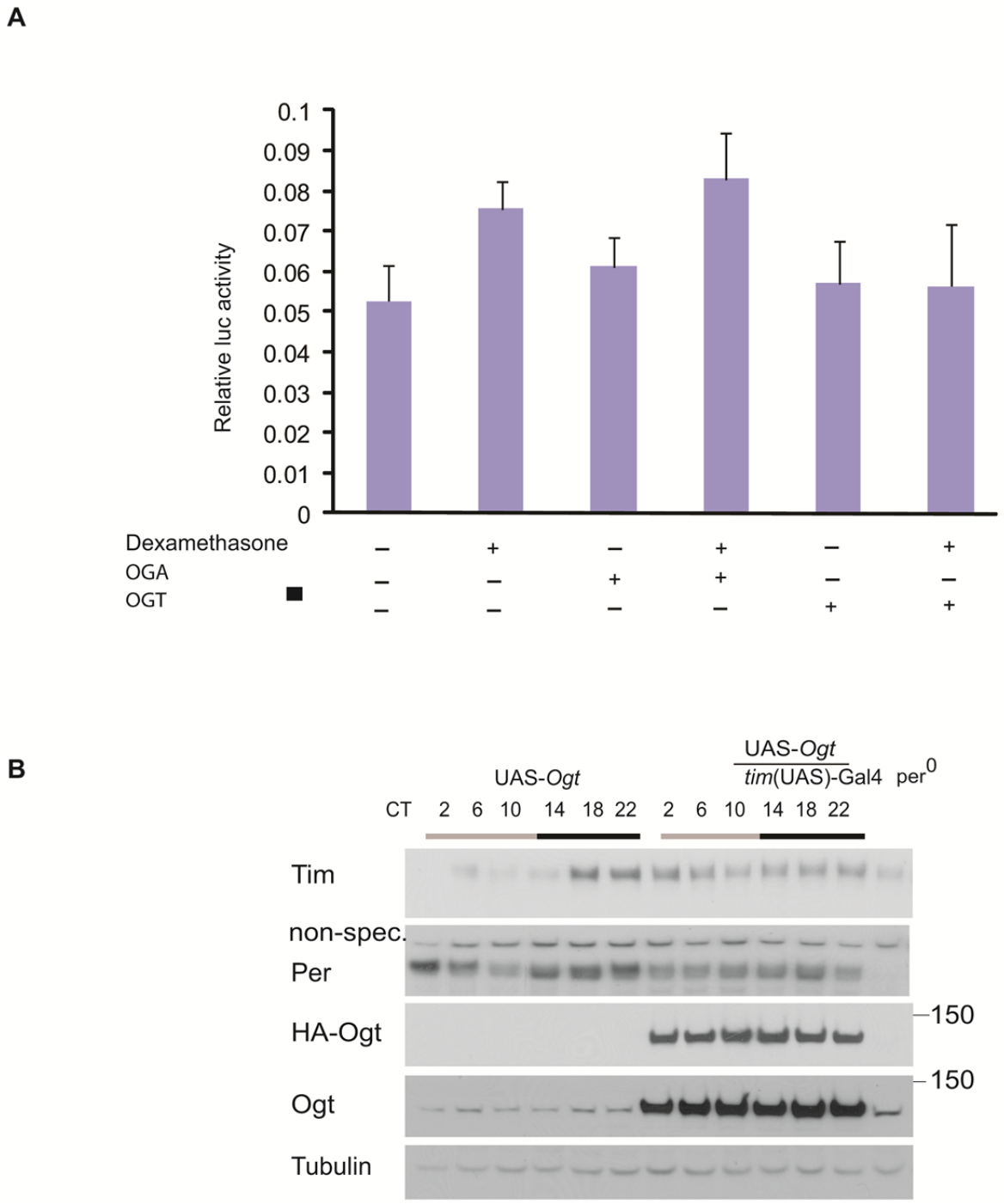

Figure S4. OGT and OGA Overexpression Specifically Alter TIM and PER Expression without Affecting RNA Polymerase II Activity, Related to Figure 5

(A) Luciferase assay with pGL3–TAT promoter construct. Addition of OGA or OGT do not significantly ($p>0.05$) alter luciferase levels, demonstrating the generic effect of *O*-GlcNAc on RNA pol II does not impact the results of luciferase activity experiments. Luciferase assays were performed in triplicate on at least three independent occasions. Error bars represent SEM. (B) Another representative blot demonstrating *Ogt* overexpression reduces Tim and Per protein expression amplitude. Non-specific band labeled as "non-spec" in second panel from top. Overexpressed Ogt was detected by HA antibody in third panel and by anti-Ogt in fourth panel from top.

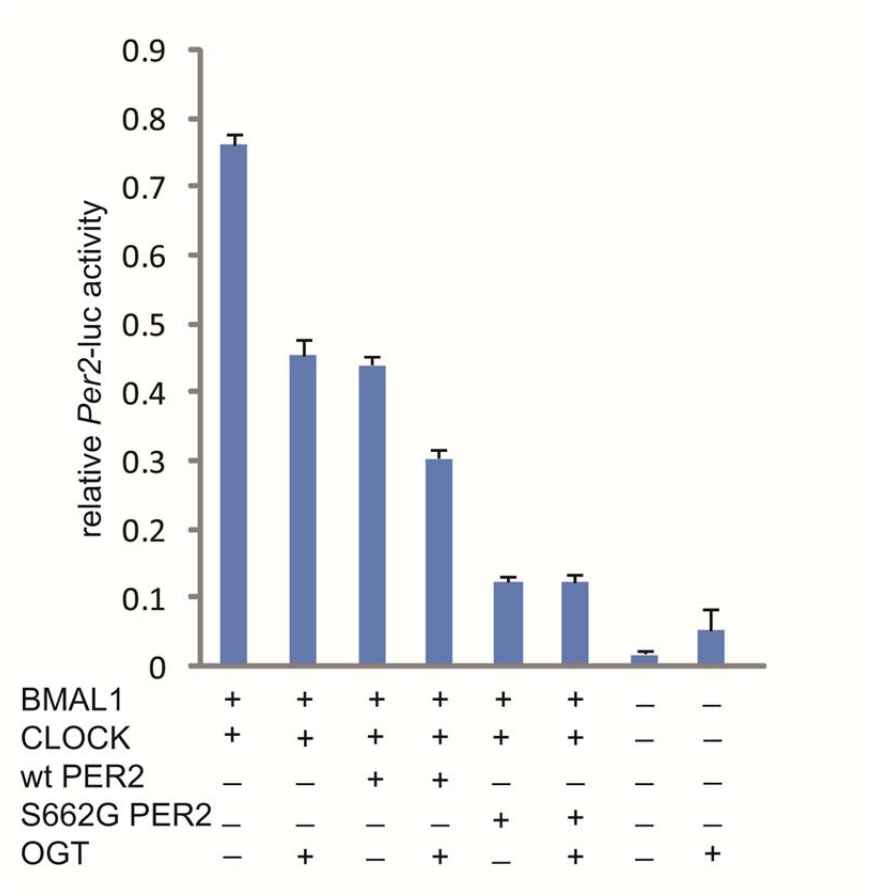

Figure S5. S662G PER2 Displays Enhanced Transcriptional Repressor Activity, Compared to WT PER2, Independent of OGT, Related to Figure 6

OGT represses *Per2*-luc activity when co-transfected with WT PER2 and does not affect *Per2*-luc activity when co-transfected with S662G PER2. S662G PER2 is stronger repressor than WT PER2. Luciferase assays were performed in triplicate on at least three independent occasions. Error bars represent SEM.

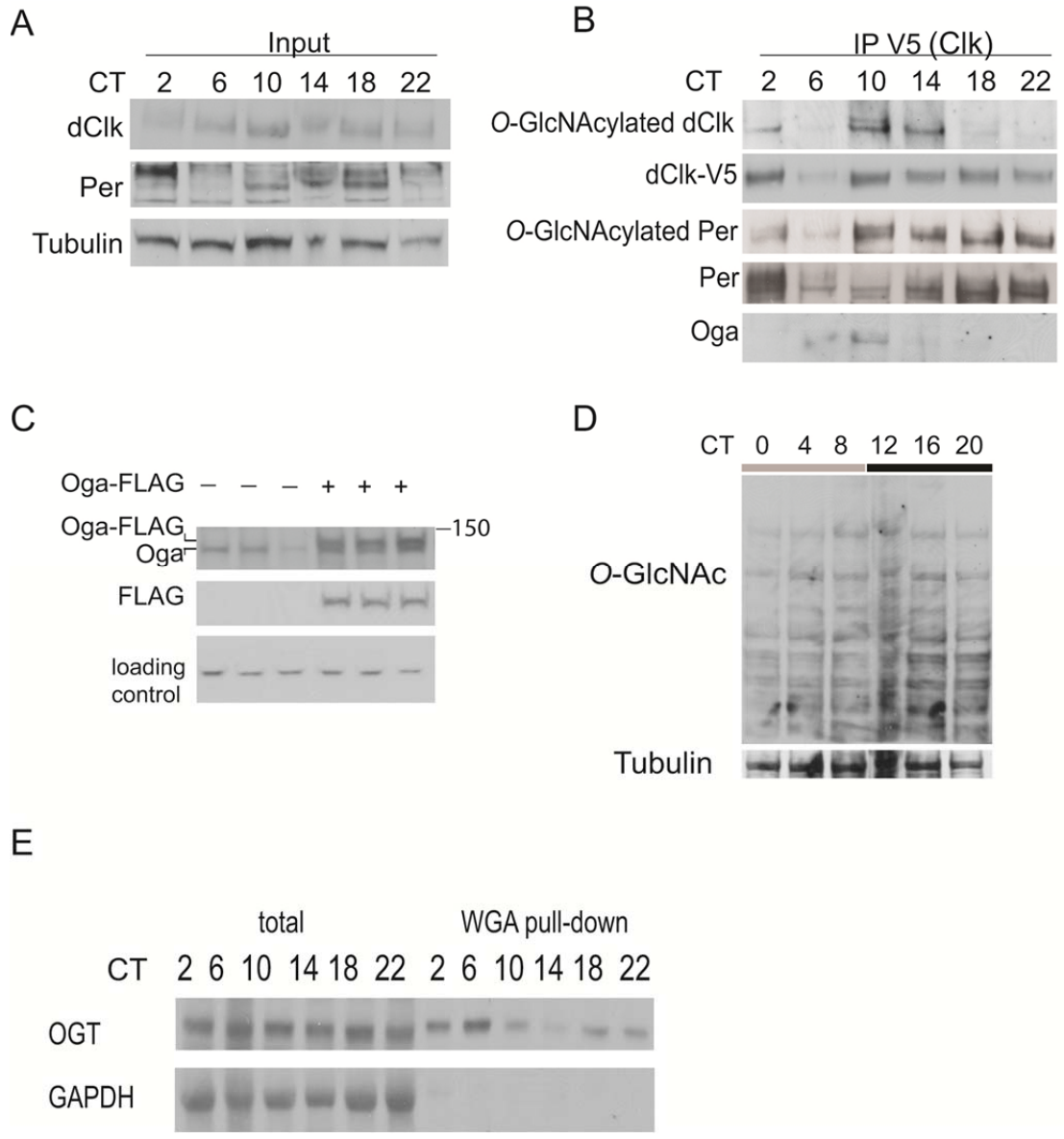

Figure S6. Circadian Oscillation of *O*–GlcNAcylation, Related to Figure 7

dClk and dPer are *O*-GlcNAc modified *in vivo* and dClk interacts with Oga. dClk was immunoprecipitated from yw;;dClk-V5 fly heads (one extra copy of Clk) every 4 hours over 24 hour circadian time as indicated. Immunoprecipitated proteins were immunoblotted with antibodies recognizing *O*-GlcNAc, dClk, dPer, and Oga. Input (A) of total protein and IP (B) are shown. Quantification of immunoprecipitated total dClk and dPer proteins and *O*-GlcNAcylated dClk and dPer proteins normalized with immunoprecipitated protein levels gave patterns over circadian time very similar to what is shown in Figure 7B (data over zeitgeber time). (C) OGA antibody recognize *Drosophila* proteins**.** S2 cells transfected with or without *Drosophila* Oga-Flag and immunoblotted with antibodies against Flag tag and OGA (Sigma Prestige or Proteinteck Group, Inc). Upper band of the upper panel indicates Oga-Flag expression while the lower band indicates endogenous Oga when the blot was probed by OGA antibody. Both OGT and OGA antibodies have previously shown to recognize mouse proteins (Capotosti et al., 2011; Keembiyehetty et al., 2011). (D) *O*-GlcNAc levels from the protein lysates extracted from the WT fly heads over circadian time course. (E) Wheat germ agglutinin (WGA) pulldown from the liver tissues of the cytoplasmic fractions over the circadian time. Wheat germ agglutinin (WGA) is a lectin with binding specificity for GlcNAc. Antibodies used to detect the total levels and WGA pulldown levels are against OGT and GAPDH.

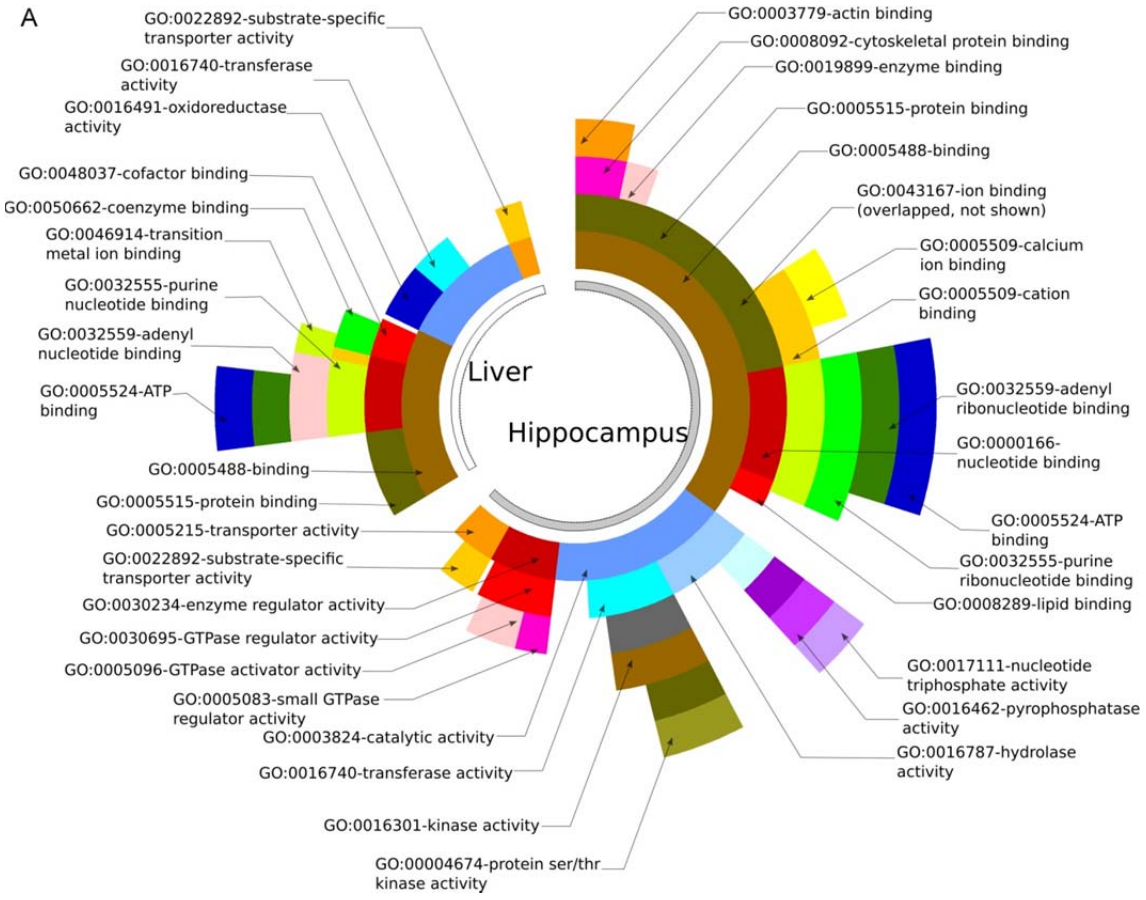
A
GO:0022892-substrate-specific transporter activity
GO:0016740-transferase activity
GO:0016491-oxidoreductase activity
GO:0048037-cofactor binding
GO:0050662-coenzyme binding
GO:0046914-transition metal ion binding
GO:0032555-purine nucleotide binding
GO:0032559-adenyl nucleotide binding
GO:0005524-ATP binding
GO:0005488-binding
GO:0005515-protein binding
GO:0005215-transporter activity
GO:0022892-substrate-specific transporter activity
GO:0030234-enzyme regulator activity
GO:0030695-GTPase regulator activity
GO:0005096-GTPase activator activity
GO:0005083-small GTPase regulator activity
GO:0003824-catalytic activity
GO:0016740-transferase activity
GO:0016301-kinase activity
GO:00004674-protein ser/thr kinase activity
Liver
Hippocampus
GO:0003779-actin binding
GO:0008092-cytoskeletal protein binding
GO:0019899-enzyme binding
GO:0005515-protein binding
GO:0005488-binding
GO:0043167-ion binding (overlapped, not shown)
GO:0005509-calcium ion binding
GO:0005509-cation binding
GO:0032559-adenyl ribonucleotide binding
GO:0000166-nucleotide binding
GO:0005524-ATP binding
GO:0032555-purine ribonucleotide binding
GO:0008289-lipid binding
GO:0017111-nucleotide triphosphate activity
GO:0016462-pyrophosphatase activity
GO:0016787-hydrolase activity

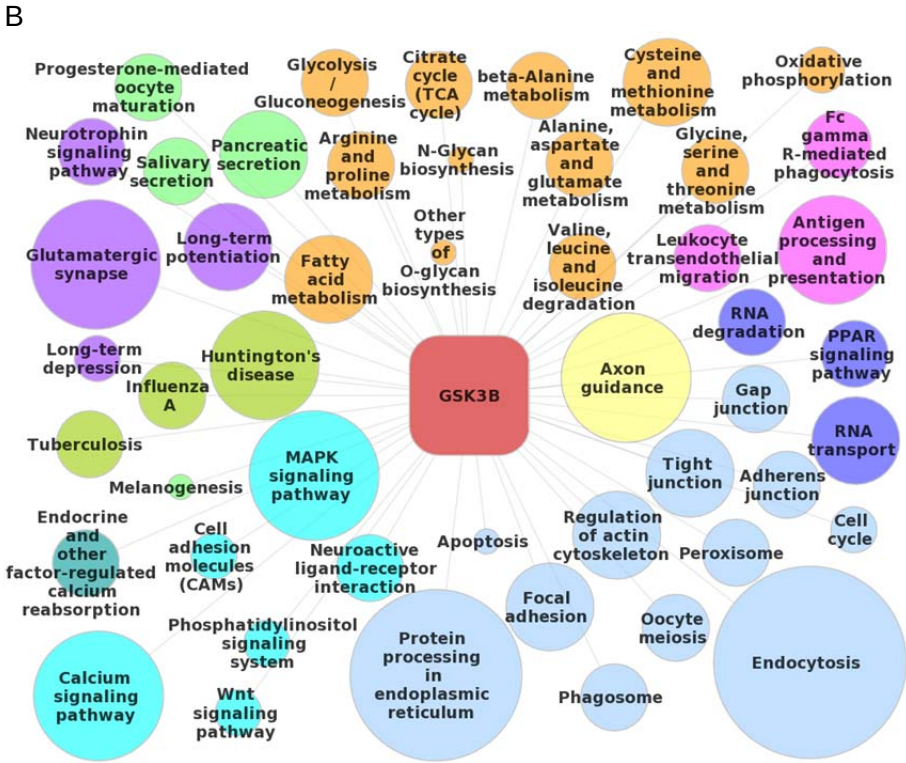
B
Progesterone-mediated oocyte maturation
Glycolysis / Gluconeogenesis
Citrate cycle (TCA cycle)
beta-Alanine metabolism
Cysteine and methionine metabolism
Oxidative phosphorylation
Neurotrophin signaling pathway
Salivary secretion
Pancreatic secretion
Arginine and proline metabolism
N-Glycan biosynthesis
Alanine, aspartate and glutamate metabolism
Glycine, serine and threonine metabolism
Fc gamma R-mediated phagocytosis
Glutamatergic synapse
Long-term potentiation
Fatty acid metabolism
Other types of O-glycan biosynthesis
Valine, leucine and isoleucine degradation
Leukocyte transendothelial migration
Antigen processing and presentation
RNA degradation
PPAR signaling pathway
Long-term depression
Influenza A
Huntington's disease
GSK3B
Axon guidance
Gap junction
RNA transport
Tuberculosis
MAPK signaling pathway
Tight junction
Adherens junction
Melanogenesis
Endocrine and other factor-regulated calcium reabsorption
Cell adhesion molecules (CAMs)
Neuroactive ligand-receptor interaction
Apoptosis
Regulation of actin cytoskeleton
Peroxisome
Cell cycle
Focal adhesion
Oocyte meiosis
Phosphatidylinositol signaling system
Protein processing in endoplasmic reticulum
Endocytosis
Calcium signaling pathway
Wnt signaling pathway
Phagosome

Figure S7. Bioinformatic Analyses of GSK3β Interacting Proteome

(A) GO analyses of GSK3β potential substrates/binding partners. Pie graphs for GO analysis of analog-specific substrates found in hippocampus only or liver only. GO entries in the inner circles are more general, while those in the outer circles are more specific. Between a pair of experiments, GO entries have the same colors in both graphs. The colors are reused every 22 unique GO entries. (B) GSK3β pathways identified with KEGG. The corresponding mouse ENTREZ protein IDs were used for searching the KEGG database. The size of the circle is proportional to the number of proteins identified from our protein list. KEGG pathways containing three or more proteins from our protein list are shown here with each circle representing one pathway. Illustrated is the *O*-Glycan biosynthesis pathway which includes OGT from our protein list. Pathways of similar types, such as metabolism or signal transduction are shown in the same background colors.

Table S4. **Locomotor Activity Rhythms of Transgenic *Drosophila* Lines Either Knocking Down or Overexpressing *Ogt* and *Oga*, Related to Figure 3**

Genotype	tau (Hours)	SEM (Hours)
tim(UAS)-Gal4 (UAS)-18610 (UAS)-Dicer2/+	21.5	0.1
tim(UAS)-Gal4 (UAS)-18611 (UAS)-Dicer2/+	22.1	0.06
tim(UAS)-Gal4 (UAS)-41822 (UAS)-Dicer2/+	23.6	0.2
tim(UAS)-Gal4 (UAS)-41823 (UAS)-Dicer2/+	24.9	0.1
(UAS)-41823	23.6	0.1
(UAS)-18610	23.5	0.09
UAS HA-ogt (100)/ *tim*(UAS)-Gal4	27.3	0.3
UAS HA-ogt (101)/ *tim*(UAS)-Gal4	26.7	0.1
UAS HA-ogt (102)/ *tim*(UAS)-Gal4	25.5	0.1
UAS HA-ogt (103/) *tim*(UAS)Gal4	26.6	0.1
UAS HA-ogt (104)/ *tim*(UAS)-Gal4	26.2	0.09
UAS HA-ogt (105)/ *tim*(UAS)-Gal4	25.7	0.2
UAS HA-ogt (106)/ *tim*(UAS)-Gal4	25.8	0.1
UAS ogt (200)/ *tim*(UAS)-Gal4	27.05	0.3
UAS ogt (201)/ *tim*(UAS)-Gal4	26.05	0.08
UAS ogt (202)/ *tim*(UAS)-Gal4	26.5	0.1
UAS ogt (203)/ *tim*(UAS)-Gal4	26.5	0.1
UAS ogt (209)/ *tim*(UAS)-Gal4	28.1	0.2
UAS ogt (210)/ *tim*(UAS)-Gal4	27.1	0.2
UAS HA-oga (300)/ *tim*(UAS)-Gal4	22.7	0.08
UAS HA-oga (301)/ *tim*(UAS)-Gal4	23	0.04
UAS HA-oga (303)/ *tim*(UAS)-Gal4	22.7	0.07
tim(UAS)-Gal4/+	23.9	0.02
UAS oga (405)/ *tim*(UAS)-Gal4	22.8	0.05
UAS oga (408)/ *tim*(UAS)-Gal4	22.9	0.05
tim(UAS)-Gal4/+	23.9	0.02

Genotypes of flies, period length (tau) in hours are shown as indicated. At least 32 flies were used for circadian activity experiment from each genotype.

Supplemental Experimental Procedures

Antibodies and Materials

Primary antibodies used in this study are: GSK3αβ (Santa Cruz, sc-7291), GSK3β (Cell Signaling), pSer9 GSK3β (Abcam), Rev-erbα (Cell Signaling), pSer55/59 Rev-erbα (Cell Signaling), ZO1 (Santa Cruz), Per2 (Alpha Diagnostic International), thioester specific antibody (Levi et al., 2007). FLAG (Sigma), V5 (Invitrogen, Sigma), V5 antibody conjugated agarose (Abcam), anti-FLAG M2 affinity gel (Sigma), c-myc 9E10 (Sigma), HA.11 (Covance), His (Novagen), Period and Timeless (Seghal lab), Clock (Houl et al., 2008), Oga (Protein Teck Group, Inc, Sigma Prestige, Santa Cruz), Ogt (Sigma, Santa Cruz), *O*-linked N-acetylglucosamine (RL2 and CDT110.6, ThermoScientific, Covance and Novus Biological), Clock (sc25361, Santa Cruz), Per2 (PER21A, Alpha Diagnostics), GAPDH (Santa Cruz), CK1δ (ab 48031 Abcam), and p662p665p668 PER2 (Shanware et al., 2011). p662PER2 antibody was made in Fu lab using p662 specific peptide (Toh et al., 2001). N-6 phenethyl and benzyl ATPγS and 1-Na-PP1 inhibitor was provided by the Shokat lab (Levi et al., 2007). 100 mM GlcNAc (Sigma) was used as competitor for *O*-GlcNAc antibody in 5% BSA TBST overnight at 4C.

Mass Spectrometry

Gel lanes were sliced into roughly twenty bands for analysis. Disulfide bonds were reduced using 10mM dithiothreitol, then alkylated using 50mM iodoacetamide, before overnight digestion with TPCK-modified trypsin (Promega). Extracted peptides were analyzed by LC-MS/MS using an Eksigent nano-LC and either a QSTAR (AB Sciex) or LTQ-FT (Thermo) mass spectrometer. Peak lists were created using the mascot.dll (for QSTAR data) or in-house PAVA software (for LTQ-FT data). Data were searched using Protein Prospector version 5.8.0. For PNBM IPs, data was searched against a concatenated database of all rodent entries in UniProt downloaded on August 10th 2010 and randomized versions of their sequences (431542 entries). For thio-ester IP data a concatenated database of human entries in UniProt downloaded on June 15th 2010 was queried (658836 entries). QSTAR data was searched allowing for a precursor mass tolerance of 100 ppm and fragment mass tolerance of 0.15 Da. LTQ-FT data was searched allowing for a precursor mass tolerance of 30 ppm and fragment mass tolerance of 0.6 Da. Cysteine residues were assumed to be carbamidomethylated, and oxidation of methionines, pyroglutamate formation from N-terminal glutamines and protein N-terminal acetylation were considered as potential modifications. Reliability of results was assessed based on the target-decoy searching strategy (Elias and Gygi, 2007), and results reported had estimated protein false discovery rates of between 1-4 %.

Data for identification of post-translational modification sites on OGT was acquired by LC-MS/MS using a Nanoacquity (Waters) UPLC system interfaced to a LTQ-Orbitrap Velos (Thermo) mass spectrometer. After a survey scan, the three most intense multiply charged peaks were selected for both HCD fragmentation (measured in the orbitrap) and ETD fragmentation (measured in the ion trap). Data were searched using Protein Prospector version 5.10.0 (Mol Cell Proteomics. 2010 9(9):1795-1803) against all human entries in UniProt downloaded on January 11th 2011, plus randomized versions of these sequences (a total of 194452 entries were queried). HCD and ETD data were searched separately. In each case the precursor mass tolerance was 20 ppm and all the modifications listed above were considered, plus additionally HexNAc modification of serine or threonine and phosphorylation of serine, threonine or tyrosine. For HCD data only, neutral loss of HexNAc (i.e. where the precursor was modified but none of the fragment ions) was also considered. For HCD data the fragment mass tolerance was set to 30 ppm; for ETD data it was set to 0.6 Da.

Bioinformatic Analyses for Identified Proteins

Gene Ontology (GO) analysis was applied to examine similarities and differences among the datasets of putative substrates/partners. For this purpose, protein lists from AS-GSK3β modified pulldown data sets

uniquely positive only from either hippocampus or liver extracts were used. The associated GO entries for these proteins were identified based on GO association information (org.Mm.eg.db) from Bioconductor (www.bioconductor.org). To visualize the overall similarities and differences (with some detail not shown) in the "induced" Gene Ontology categories between pairwise experiments, we used graphic software - Circos (http://mkweb.bcgsc.ca/circos/) to draw pie graphs (File. S3A).

Based on Gene Set Enrichment Analysis, those GO entries that are over-represented in an experiment compared to the universal distribution were identified and are shown. For clarity, only GO entries with p-value <0.05 and containing more than 5 genes from our lists are shown. For more complete information, the text based GO tree files can be found in the supplementary files. Because the purpose of these graphs is to highlight the similarities and differences between pairwise experiments, some intermediate layers of GO entries are not shown if they overlap with other GO entries. As shown in File S3A, many proteins are of the same GO entries between the pairwise experiments (such as GO:0022892 for hippocampus/liver) and many unique ones are also found (including GO:0030695 for hippocampus vs. liver). For example, the "GO:0030695-GTPase regulatory activity" category is one of the most obvious differences in Gene Ontology between the hippocampus and liver results. The genes belong to GO:0030695 that are identified in hippocampus but not in liver include Ras GTPase activating proteins, Rho/Rac guanine nucleotide exchange factors and SLIT-ROBO Rho GTPase activating proteins (see Supplemental File S1).

Proteins identified in the AS-GSK3β hippocampus positive only and AS-GSK3β liver positive only were further examined in the KEGG database (http://www.genome.jp/kegg) to identify pathways that may be regulated by GSK3β. The corresponding mouse ENTREZ protein IDs were used for searching the KEGG database. KEGG pathways containing three or more proteins from our protein list are shown here (File S3B) with each circle representing one pathway.

Analog-Specific Kinase Procedures

Fresh mouse hippocampal or liver tissues extracted at different circadian times were used for kinase reactions. Saponin (Sigma, 10μg/ml) was added to the 1XGSK3 kinase buffer with complete protease inhibitors (Roche) and phosphatase inhibitors I and II (Sigma) to permeabilize cell membranes. Tissues were homogenized manually. Reactions were supplied with either AS-GSK3β or WT-GSK3β, 2mM GTP, 0.1mM ATP and 0.2mM N6-phenethyl ATPγS and were performed at room temperature for 15 min. After kinase assays, 2X RIPA buffer (100mM Hepes pH 7.8, 300mM NaCl, 2.0 % NP-40, 0.2 % SDS, 20mM EDTA) with 1.5 mM PNBM was added and samples were incubated at 4°C with rocking for 2 hrs. PNBM was removed by size exclusion column PD-10 (Amersham Pharmacia). Protein lysates were pre-cleared by G-Sepharose for 2 hrs (0.8mg/ml) and protein concentrations were measured with the Bradford method (Pierce). Proteins (0.8mg/ml) were immunoprecipitated with approximately 30 μg/ml thiophosphate ester specific antibody at 4°C for 12-16 hrs and BSA pre-blocked protein G-Sepharose (GE Healthcare) was added for 2 hrs. Beads were then washed 4 times with 1X RIPA and proteins were separated on 4-15% SDS-PAGE (Invitrogen), stained with Colloidal Coomassie (Invitrogen) and analyzed by mass spectrometry.

Mapping of Phosphorylation and *O*-GlcNAcylation Sites

Full-length hOGT (OriGene) or OGT-FLAG were transfected and purified using FLAG affinity tag from HEK293 cells and phosphorylated by GSK3β (Biolabs) *in vitro*.

WGA Lectin Pulldown

Liver tissues were lysed and cytoplamic fractions were extracted using Pierce cytoplasmic fraction extraction reagensts. For WGA pulldown 100 ug of protein was used (Vector Laboratories Inc.).

Plasmid Constructs

The coding region of GSK3β was cloned into the pGEX-6P plasmid at the Bgl II/ Not I site (GE Healthcare). AS-GSK3β was generated by mutating the "gatekeeper" residue (L132) to A or G with the site-directed Quick-Change kit from Stratagene. Both alleles were used for *in vitro* kinase assays. The L132G GSK3β allele was used for the GSK3β proteomic screen with mouse tissues because of its higher affinity for the ATPγS analog. AS-GSK3β was cloned into the pGLUE tandem-affinity purification plasmid (Angers et al., 2006). Clones of *Ogt* (SD06381) and *Oga* (RE69909) were obtained from FlyBase. *Ogt* and *Oga* cDNAs were cloned by PCR into the pUAST plasmid to include an HA tag. UAS-*Ogt* and UAS-*Oga* transgenic flies were generated using clones with or without a N-terminal HA tag. For S2 cell expression, *Ogt*, *Oga*, *Per*, *Cyc*, and *Dbt* were first cloned into the pENTR plasmid (Invitrogen) and fly Gateway plasmids were then obtained from the Carnegie Institution. *Oga* and *Ogt* were cloned into pAFW; *Per* was cloned into pAMW. *Cyc* and *Dbt* were cloned into the pAHW plasmid. d*Clk-V5* (Menet et al., 2010) and *Tim* constructs were previously published (Kivimae et al., 2008). For HEK293 expression, clones of mouse *OGT* and *OGA* were obtained from Open Biosystem and cloned into the p3XFLAG-CMV-10 plasmid (Sigma) or pcDNA6.2/V5/GW/D-TOPO (Invitrogen). Site-directed Quick-Change kit from Stratagene was used to generate S3AS4A OGT or S3DS4D OGt. ptGFPN1-h*PER2*-myc (Xu et al., 2007) and pcDNA 3.1-*Clock*-Flag (Kaasik and Lee, 2004) were used. h*PER2* was cloned into p3XFLAG-CMV-10 plasmid (Sigma). 7.2 kb *PER2* promoter were previously published *(34)*. All clones were confirmed by DNA sequencing. Coding region of GSK3β was amplified by PCR using oligonucleotides (F)- CGGAGATCTATGTCGGGGCGACCGAGAACCAC and (R)-CTAGCGGCCGCTCAGGTGGAGTTGGAAGCTGATGCA. All the other used oligo sequences are available upon request.

Western Blot and Immunoprecipitation from Fly Heads

Goat polyclonal V5-agarose (Abcam) was used to immunoprecipitate Clk from yw;; Clk-V5 flies over circadian time. The IP protocol was adapted from a previous report (Menet et al., 2010) with some modification and 100μM PUGNAc was included in the lysis solution.

RNA Isolation and q-PCR

Total RNAs were isolated from fly heads with TRIzol and further purified using RNAeasy columns (Qiagen). cDNAs were synthesized using Thermoscript III, and q-PCR was performed using SYBR Green according to the manufacture's protocol (ABI). Oligos for q-PCR were adapted from previous reports (Kadener et al., 2008; Kilman et al., 2009). mRNA values from fly heads were normalized to ribosomal protein 49 (*rp49*).

SUPPLEMENTAL REFERENCES

Capotosti, F., Guernier, S., Lammers, F., Waridel, P., Cai, Y., Jin, J., Conaway, J.W., Conaway, R.C., and Herr, W. (2011). O-GlcNAc transferase catalyzes site-specific proteolysis of HCF-1. Cell *144*, 376-388.

Elias, J.E., and Gygi, S.P. (2007). Target-decoy search strategy for increased confidence in large-scale protein identifications by mass spectrometry. Nat Methods *4*, 207-214.

Houl, J.H., Ng, F., Taylor, P., and Hardin, P.E. (2008). CLOCK expression identifies developing circadian oscillator neurons in the brains of Drosophila embryos. BMC Neurosci *9*, 119.

Keembiyehetty, C.N., Krzeslak, A., Love, D.C., and Hanover, J.A. (2011). A lipid-droplet-targeted O-GlcNAcase isoform is a key regulator of the proteasome. J Cell Sci *124*, 2851-2860.

Levi, F., Focan, C., Karaboue, A., de la Valette, V., Focan-Henrard, D., Baron, B., Kreutz, F., and Giacchetti, S. (2007). Implications of circadian clocks for the rhythmic delivery of cancer therapeutics. Adv Drug Deliv Rev *59*, 1015-1035.

Shanware, N.P., Hutchinson, J.A., Kim, S.H., Zhan, L., Bowler, M.J., and Tibbetts, R.S. (2011). Casein kinase 1-dependent phosphorylation of familial advanced sleep phase syndrome-associated residues controls PERIOD 2 stability. J Biol Chem *286*, 12766-12774.

Toh, K.L., Jones, C.R., He, Y., Eide, E.J., Hinz, W.A., Virshup, D.M., Ptacek, L.J., and Fu, Y.H. (2001). An hPer2 phosphorylation site mutation in familial advanced sleep phase syndrome. Science *291*, 1040-1043.

Angers, S., Thorpe, C.J., Biechele, T.L., Goldenberg, S.J., Zheng, N., MacCoss, M.J., and Moon, R.T. (2006). The KLHL12-Cullin-3 ubiquitin ligase negatively regulates the Wnt-beta-catenin pathway by targeting Dishevelled for degradation. Nat Cell Biol *8*, 348-357.

Capotosti, F., Guernier, S., Lammers, F., Waridel, P., Cai, Y., Jin, J., Conaway, J.W., Conaway, R.C., and Herr, W. (2011). O-GlcNAc transferase catalyzes site-specific proteolysis of HCF-1. Cell *144*, 376-388.

Elias, J.E., and Gygi, S.P. (2007). Target-decoy search strategy for increased confidence in large-scale protein identifications by mass spectrometry. Nat Methods *4*, 207-214.

Houl, J.H., Ng, F., Taylor, P., and Hardin, P.E. (2008). CLOCK expression identifies developing circadian oscillator neurons in the brains of Drosophila embryos. BMC Neurosci *9*, 119.

Kaasik, K., and Lee, C.C. (2004). Reciprocal regulation of haem biosynthesis and the circadian clock in mammals. Nature *430*, 467-471.

Kadener, S., Menet, J.S., Schoer, R., and Rosbash, M. (2008). Circadian transcription contributes to core period determination in Drosophila. PLoS Biol *6*, e119.

Keembiyehetty, C.N., Krzeslak, A., Love, D.C., and Hanover, J.A. (2011). A lipid-droplet-targeted O-GlcNAcase isoform is a key regulator of the proteasome. J Cell Sci *124*, 2851-2860.

Kilman, V.L., Zhang, L., Meissner, R.A., Burg, E., and Allada, R. (2009). Perturbing dynamin reveals potent effects on the Drosophila circadian clock. PLoS One *4*, e5235.

Kivimae, S., Saez, L., and Young, M.W. (2008). Activating PER repressor through a DBT-directed phosphorylation switch. PLoS Biol *6*, e183.

Levi, F., Focan, C., Karaboue, A., de la Valette, V., Focan-Henrard, D., Baron, B., Kreutz, F., and Giacchetti, S. (2007). Implications of circadian clocks for the rhythmic delivery of cancer therapeutics. Adv Drug Deliv Rev *59*, 1015-1035.

Menet, J.S., Abruzzi, K.C., Desrochers, J., Rodriguez, J., and Rosbash, M. (2010). Dynamic PER repression mechanisms in the Drosophila circadian clock: from on-DNA to off-DNA. Genes Dev *24*, 358-367.

Shanware, N.P., Hutchinson, J.A., Kim, S.H., Zhan, L., Bowler, M.J., and Tibbetts, R.S. (2011). Casein kinase 1-dependent phosphorylation of familial advanced sleep phase syndrome-associated residues controls PERIOD 2 stability. J Biol Chem *286*, 12766-12774.

Toh, K.L., Jones, C.R., He, Y., Eide, E.J., Hinz, W.A., Virshup, D.M., Ptacek, L.J., and Fu, Y.H. (2001). An hPer2 phosphorylation site mutation in familial advanced sleep phase syndrome. Science *291*, 1040-1043.

Xu, Y., Toh, K.L., Jones, C.R., Shin, J.Y., Fu, Y.H., and Ptacek, L.J. (2007). Modeling of a human circadian mutation yields insights into clock regulation by PER2. Cell *128*, 59-70.